Collier, D.A., Barrett, T.G., Curtis, D., Macleod, A., Arranz, M.J., Maassen, J.A., Bundey, S., 1996. Linkage of Wolfram syndrome to chromosome 4p16.1 and evidence for heterogeneity. Am. J. Hum. Genet. 59, 855–863.

Condé, F., Maire-Lepoivre, E., Audinat, E., Crépel, F., 1995. Afferent connections of the medial frontal cortex of the rat. II. Cortical and subcortical afferents. J. Comp. Neurol. 352, 567–593.

Crick, F., 1984. Function of the thalamic reticular complex: the searchlight hypothesis. Proc. Natl. Acad. Sci. U.S.A. 81, 4586–4590.

Cryns, K., Thys, S., Van Laer, L., Oka, Y., Pfister, M., Van Nassauw, L., Smith, R.J., Timmermans, J.P., Van Camp, G., 2003. The *WFS1* gene, responsible for low frequency sensorineural hearing loss and Wolfram syndrome, is expressed in a variety of inner ear cells. Histochem. Cell Biol. 119, 247–256.

de Olmos, J., Hardy, H., Heimer, L., 1978. The afferent connections of the main and the accessory olfactory bulb formations in the rat: an experimental HRP-study. J. Comp. Neurol. 181, 213–244.

de Olmos, J.S., Beltramino, C.A., Alheid, G., 2004. Amygdala and extended amygdala of the rat: a cytoarchitectonical, fibroarchitectonical, and chemoarchitectonical survey. In: Paxinos, G. (Ed.), The Rat Nervous System. third ed. Elsevier Academic Press, San Diego, pp. 509–603.

Desban, M., Kemel, M.L., Glowinski, J., Gauchy, C., 1993. Spatial organization of patch and matrix compartments in the rat striatum. Neuroscience 57, 661–671.

Eid, T., Jorritsma-Byham, B., Schwarcz, R., Witter, M.P., 1996. Afferents to the seizure-sensitive neurons in layer III of the medial entorhinal area: a tracing study in the rat. Exp. Brain Res. 109, 209–218.

Evans, K.L., Lawson, D., Meitinger, T., Blackwood, D.H., Porteous, D.J., 2000. Mutational analysis of the Wolfram syndrome gene in two families with chromosome 4p-linked bipolar affective disorder. Am. J. Med. Genet. 96, 158–160.

Fonnum, F., 1970. Topographical and subcellular localization of choline acetyltransferase in rat hippocampal region. J. Neurochem. 17, 1029–1037.

Fonseca, S.G., Fukuma, M., Lipson, K.L., Nguyen, L.X., Allen, J.R., Oka, Y., Urano, F., 2005. WFS1 is a novel component of the unfolded protein response and maintains homeostasis of the endoplasmic reticulum in pancreatic β-cells. J. Biol. Chem. 280, 39609–39615.

Furlong, R.A., Ho, L.W., Rubinsztein, J.S., Michael, A., Walsh, C., Paykel, E.S., Rubinsztein, D.C., 1999. A rare coding variant within the *wolframin* gene in bipolar and unipolar affective disorder cases. Neurosci. Lett. 277, 123–126.

Gabreëls, B.A., Swaab, D.F., de Kleijn, D.P., Dean, A., Seidah, N.G., Van de Loo, J.W., Van de Ven, W.J., Martens, G.J., Van Leeuwen, F.W., 1998. The vasopressin precursor is not processed in the hypothalamus of Wolfram syndrome patients with diabetes insipidus: evidence for the involvement of PC2 and 7B2. J. Clin. Endocrinol. Metab. 83, 4026–4033.

Gabriel, M., Foster, K., Orona, E., 1980. Interaction of laminae of the cingulate cortex with the anteroventral thalamus during behavioral learning. Science 208, 1050–1052.

Genís, D., Dávalos, A., Molins, A., Ferrer, I., 1997. Wolfram syndrome: a neuropathological study. Acta Neuropathol. (Berl.) 93, 426–429.

Goto, M., Swanson, L.W., Canteras, N.S., 2001. Connections of the nucleus incertus. J. Comp. Neurol. 438, 86–122.

Groenewegen, H.J., Witter, M.P., 2004. Thalamus. In: Paxinos, G. (Ed.), The Rat Nervous System. third ed. Elsevier Academic Press, San Diego, pp. 407–453.

Guillery, R.W., Feig, S.L., Lozsádi, D.A., 1998. Paying attention to the thalamic reticular nucleus. Trends Neurosci. 21, 28–32.

Gómez-Zaera, M., Strom, T.M., Rodríguez, B., Estivill, X., Meitinger, T., Nunes, V., 2001. Presence of a major WFS1 mutation in Spanish Wolfram syndrome pedigrees. Mol. Genet. Metab. 72, 72–81.

Haberly, L.B., Price, J.L., 1978. Association and commissural fiber systems of the olfactory cortex of the rat. J. Comp. Neurol. 178, 711–740.

Haglund, L., Swanson, L.W., Köhler, C., 1984. The projection of the supramammillary nucleus to the hippocampal formation: an immunohistochemical and anterograde transport study with the lectin PHA-L in the rat. J. Comp. Neurol. 229, 171–185.

Hardy, C., Khanim, F., Torres, R., Scott-Brown, M., Seller, A., Poulton, J., Collier, D., Kirk, J., Polymeropoulos, M., Latif, F., Barrett, T., 1999. Clinical and molecular genetic analysis of 19 Wolfram syndrome kindreds demonstrating a wide spectrum of mutations in WFS1. Am. J. Hum. Genet. 65, 1279–1290.

Herkenham, M., 1978. The connections of the nucleus reuniens thalami: evidence for a direct thalamo-hippocampal pathway in the rat. J. Comp. Neurol. 177, 589–610.

Hofmann, S., Philbrook, C., Gerbitz, K.D., Bauer, M.F., 2003. Wolfram syndrome: structural and functional analyses of mutant and wild-type wolframin, the WFS1 gene product. Hum. Mol. Genet. 12, 2003–2012.

Inoue, H., Tanizawa, Y., Wasson, J., Behn, P., Kalidas, K., Bernal-Mizrachi, E., Mueckler, M., Marshall, H., Donis-Keller, H., Crock, P., Rogers, D., Mikuni, M., Kumashiro, H., Higashi, K., Sobue, G., Oka, Y., Permutt, M.A., 1998. A gene encoding a transmembrane protein is mutated in patients with diabetes mellitus and optic atrophy (Wolfram syndrome). Nat. Genet. 20, 143–148.

Insausti, R., Herrero, M.T., Witter, M.P., 1997. Entorhinal cortex of the rat: cytoarchitectonic subdivisions and the origin and distribution of cortical efferents. Hippocampus 7, 146–183.

Ishihara, H., Takeda, S., Tamura, A., Takahashi, R., Yamaguchi, S., Takei, D., Yamada, T., Inoue, H., Soga, H., Katagiri, H., Tanizawa, Y., Oka, Y., 2004. Disruption of the *WFS1* gene in mice causes progressive β-cell loss and impaired stimulus-secretion coupling in insulin secretion. Hum. Mol. Genet. 13, 1159–1170.

Ishizuka, N., Weber, J., Amaral, D.G., 1990. Organization of intrahippocampal projections originating from CA3 pyramidal cells in the rat. J. Comp. Neurol. 295, 580–623.

Ito, S., Sakakibara, R., Hattori, T., 2007. Wolfram syndrome presenting marked brain MR imaging abnormalities with few neurologic abnormalities. AJNR Am. J. Neuroradiol. 28, 305–306.

Joel, D., Weiner, I., 2000. The connections of the dopaminergic system with the striatum in rats and primates: an analysis with respect to the functional and compartmental organization of the striatum. Neuroscience 96, 451–474.

Kandel, E.R., 2000. Disorders of mood: depression, mania, and anxiety disorders. In: Kandel, E.R., Schwartz, J.H., Jessell, T.M. (Eds.), Principles of Neural Science. fourth ed. McGraw-Hill, New York, pp. 1209–1226.

Kato, T., Ishiwata, M., Yamada, K., Kasahara, T., Kakiuchi, C., Iwamoto, K., Kawamura, K., Ishihara, H., Oka, Y., 2008. Behavioral and gene expression analyses of Wfs1 knockout mice as a possible animal model of mood disorder. Neurosci. Res. 61, 143–158.

Kato, T., Iwamoto, K., Washizuka, S., Mori, K., Tajima, O., Akiyama, T., Nanko, S., Kunugi, H., Kato, N., 2003. No association of mutations and mRNA expression of WFS1/wolframin with bipolar disorder in humans. Neurosci. Lett. 338, 21–24.

Kawamoto, T., Horikawa, Y., Tanaka, T., Kabe, N., Takeda, J., Mikuni, M., 2004. Genetic variations in the WFS1 gene in Japanese with type 2 diabetes and bipolar disorder. Mol. Genet. Metab. 82, 238–245.

Kawano, J., Tanizawa, Y., Shinoda, K., 2008. Wolfram syndrome 1 (*Wfs1*) gene expression in the normal mouse visual system. J. Comp. Neurol. 510, 1–23.

Kemppainen, S., Jolkkonen, E., Pitkänen, A., 2002. Projections from the posterior cortical nucleus of the amygdala to the hippocampal formation and parahippocampal region in rat. Hippocampus 12, 735–755.

Kesner, Y., Zohar, J., Merenlender, A., Gispan, I., Shalit, F., Yadid, G., 2007. *WFS1* gene as a putative biomarker for development of post-traumatic syndrome in an animal model. Mol. Psychiatry. Advance online publication on October 30, 2007. doi:10.1038/sj.mp.4002109.

Khanim, F., Kirk, J., Latif, F., Barrett, T.G., 2001. WFS1/wolframin mutations, Wolfram syndrome, and associated diseases. Hum. Mutat. 17, 357–367.

Kincaid, A.E., Wilson, C.J., 1996. Corticostriatal innervation of the patch and matrix in the rat neostriatum. J. Comp. Neurol. 374, 578–592.

Kjelstrup, K.G., Tuvnes, F.A., Steffenach, H.A., Murison, R., Moser, E.I., Moser, M.B., 2002. Reduced fear expression after lesions of the ventral hippocampus. Proc. Natl. Acad. Sci. U.S.A. 99, 10825–10830.

Klink, R., Alonso, A., 1997. Muscarinic modulation of the oscillatory and repetitive firing properties of entorhinal cortex layer II neurons. J. Neurophysiol. 77, 1813–1828.

Kosel, K.C., Van Hoesen, G.W., West, J.R., 1981. Olfactory bulb projections to the parahippocampal area of the rat. J. Comp. Neurol. 198, 467–482.

Köhler, C., 1985. Intrinsic projections of the retrohippocampal region in the rat brain. I. The subicular complex. J. Comp. Neurol. 236, 504–522.

Köhler, C., 1986. Intrinsic connections of the retrohippocampal region in the rat brain. II. The medial entorhinal area. J. Comp. Neurol. 246, 149–169.

Köhler, C., 1988. Intrinsic connections of the retrohippocampal region in the rat brain. III. The lateral entorhinal area. J. Comp. Neurol. 271, 208–228.

Köhler, C., Chan-Palay, V., Steinbusch, H., 1981. The distribution and orientation of serotonin fibers in the entorhinal and other retrohippocampal areas. An immunohistochemical study with anti-serotonin antibodies in the rats brain. Anat. Embryol. (Berl.) 161, 237–264.

Köhler, C., Steinbusch, H., 1982. Identification of serotonin and non-serotonin-containing neurons of the mid-brain raphe projecting to the entorhinal area and the hippocampal formation. A combined immunohistochemical and fluorescent retrograde tracing study in the rat brain. Neuroscience 7, 951–975.

LeDoux, J., 2007. The amygdala. Curr. Biol. 17, R868–R874.

Loewy, A.D., Spyer, K.M. (Eds.), 1990. Central Regulation of Autonomic Function. Oxford University Press, New York.

Luuk, H., Koks, S., Plaas, M., Hannibal, J., Rehfeld, J.F., Vasar, E., 2008. Distribution of Wfs1 protein in the central nervous system of the mouse and its relation to clinical symptoms of the Wolfram syndrome. J. Comp. Neurol. 509, 642–660.

McAlonan, K., Brown, V.J., Bowman, E.M., 2000. Thalamic reticular nucleus activation reflects attentional gating during classical conditioning. J. Neurosci. 20, 8897–8901.

Middle, F., Jones, I., McCandless, F., Barrett, T., Khanim, F., Owen, M.J., Lendon, C., Craddock, N., 2000. Bipolar disorder and variation at a common polymorphism (A1832G) within exon 8 of the Wolfram gene. Am. J. Med. Genet. 96, 154–157.

Minton, J.A., Hattersley, A.T., Owen, K., McCarthy, M.I., Walker, M., Latif, F., Barrett, T., Frayling, T.M., 2002. Association studies of genetic variation in the *WFS1* gene and type 2 diabetes in U.K. populations. Diabetes 51, 1287–1290.

Minton, J.A., Rainbow, L.A., Ricketts, C., Barrett, T.G., 2003. Wolfram syndrome. Rev. Endocr. Metab. Disord. 4, 53–59.

Mitrofanis, J., 1992. Calbindin immunoreactivity in a subset of cat thalamic reticular neurons. J. Neurocytol. 21, 495–505.

Moore, R.Y., Ziegler, B., Bayer, S.A., 1978. Monoamine neuron innervation of the hippocampal formation: alteration by neonatal irradiation. Exp. Neurol. 60, 318–326.

Moser, E., Moser, M.B., Andersen, P., 1993. Spatial learning impairment parallels the magnitude of dorsal hippocampal lesions, but is hardly present following ventral lesions. J. Neurosci. 13, 3916–3925.

Naber, P.A., Caballero-Bleda, M., Jorritsma-Byham, B., Witter, M.P., 1997. Parallel input to the hippocampal memory system through peri- and postrhinal cortices. Neuroreport 8, 2617–2621.

Ohtsuki, T., Ishiguro, H., Yoshikawa, T., Arinami, T., 2000. *WFS1* gene mutation search in depressive patients: detection of five missense polymorphisms but no association with depression or bipolar affective disorder. J. Affect. Disord. 58, 11–17.

Osman, A.A., Saito, M., Makepeace, C., Permutt, M.A., Schlesinger, P., Mueckler, M., 2003. Wolframin expression induces novel ion channel activity in endoplasmic reticulum membranes and increases intracellular calcium. J. Biol. Chem. 278, 52755–52762.

Palomero-Gallagher, N., Zilles, K., 2004. Isocortex. In: Paxinos, G. (Ed.), The Rat Nervous System. third ed. Elsevier Academic Press, San Diego, pp. 729–757.

Paxinos, G., Franklin, K.B.J., 2001. The Mouse Brain in Stereotaxic Coordinates, second ed. Academic Press, San Diego.

Petrovich, G.D., Risold, P.Y., Swanson, L.W., 1996. Organization of projections from the basomedial nucleus of the amygdala: a PHAL study in the rat. J. Comp. Neurol. 374, 387–420.

Pikkarainen, M., Rönkkö, S., Savander, V., Insausti, R., Pitkänen, A., 1999. Projections from the lateral, basal, and accessory basal nuclei of the amygdala to the hippocampal formation in rat. J. Comp. Neurol. 403, 229–260.

Pitkänen, A., Pikkarainen, M., Nurminen, N., Ylinen, A., 2000. Reciprocal connections between the amygdala and the hippocampal formation, perirhinal cortex, and postrhinal cortex in rat. A review. Ann. NY Acad. Sci. 911, 369–391.

Polymeropoulos, M.H., Swift, R.G., Swift, M., 1994. Linkage of the gene for Wolfram syndrome to markers on the short arm of chromosome 4. Nat. Genet. 8, 95–97.

Price, J.L., Russchen, F.T., Amaral, D.G., 1987. The limbic region. II. The amygdaloid complex. In: Björklund, A., Hökfelt, T., Swanson, L.W. (Eds.), Handbook of Chemical Neuroanatomy. Elsevier, Amsterdam, pp. 279–389.

Rando, T.A., Horton, J.C., Layzer, R.B., 1992. Wolfram syndrome: evidence of a diffuse neurodegenerative disease by magnetic resonance imaging. Neurology 42, 1220–1224.

Ribak, C.E., Vaughn, J.E., Saito, K., 1978. Immunocytochemical localization of glutamic acid decarboxylase in neuronal somata following colchicine inhibition of axonal transport. Brain Res. 140, 315–332.

Risold, P.Y., 2004. The septal region. In: Paxinos, G. (Ed.), The Rat Nervous System. third ed. Elsevier Academic Press, San Diego, pp. 605–632.

Saper, C.B., 2000. Brain stem, reflexive behavior, and the cranial nerves. In: Kandel, E.R., Schwartz, J.H., Jessell, T.M. (Eds.), Principles of Neural Science. fourth ed. McGraw-Hill, New York, pp. 873–888.

Scolding, N.J., Kellar-Wood, H.F., Shaw, C., Shneerson, J.M., Antoun, N., 1996. Wolfram syndrome: hereditary diabetes mellitus with brainstem and optic atrophy. Ann. Neurol. 39, 352–360.

Sefton, A.J., Dreher, B., Harvey, A., 2004. Visual system. In: Paxinos, G. (Ed.), The Rat Nervous System. third ed. Elsevier Academic Press, San Diego, pp. 1083–1165.

Sequeira, A., Kim, C., Seguin, M., Lesage, A., Chawky, N., Desautels, A., Tousignant, M., Vanier, C., Lipp, O., Benkelfat, C., Rouleau, G., Turecki, G., 2003. Wolfram syndrome and suicide: evidence for a role of WFS1 in suicidal and impulsive behavior. Am. J. Med. Genet. B Neuropsychiatr. Genet. 119B, 108–113.

Shannon, P., Becker, L., Deck, J., 1999. Evidence of widespread axonal pathology in Wolfram syndrome. Acta Neuropathol. (Berl.) 98, 304–308.

Shibata, H., 1993. Direct projections from the anterior thalamic nuclei to the retrohippocampal region in the rat. J. Comp. Neurol. 337, 431–445.

Shipley, M.T., Ennis, M., Puche, A.C., 2004. Olfactory system. In: Paxinos, G. (Ed.), The Rat Nervous System. third ed. Elsevier Academic Press, San Diego, pp. 923–964.

Sparsø, T., Andersen, G., Albrechtsen, A., Jørgensen, T., Borch-Johnsen, K., Sandbæk, A., Lauritzen, T., Wasson, J., Permutt, M.A., Glaser, B., Madsbad, S., Pedersen, O., Hansen, T., 2008. Impact of polymorphisms in *WFS1* on prediabetic phenotypes in a population-based sample of middle-aged people with normal and abnormal glucose regulation. Diabetologia 51, 1646–1652.

Strom, T.M., Hörtnagel, K., Hofmann, S., Gekeler, F., Scharfe, C., Rabl, W., Gerbitz, K.D., Meitinger, T., 1998. Diabetes insipidus, diabetes mellitus, optic atrophy and deafness (DIDMOAD) caused by mutations in a novel gene (*wolframin*) coding for a predicted transmembrane protein. Hum. Mol. Genet. 7, 2021–2028.

Swanson, L.W., Köhler, C., Björklund, A., 1987. The limbic region. I. The septohippocampal system. In: Björklund, A., Hökfelt, T., Swanson, L.W. (Eds.), Handbook of Chemical Neuroanatomy. Elsevier, Amsterdam, pp. 125–227.

Swanson, L.W., Wyss, J.M., Cowan, W.M., 1978. An autoradiographic study of the organization of intrahippocampal association pathways in the rat. J. Comp. Neurol. 181, 681–715.

Swift, M., Swift, R.G., 2005. Wolframin mutations and hospitalization for psychiatric illness. Mol. Psychiatry 10, 799–803.

Swift, R.G., Sadler, D.B., Swift, M., 1990. Psychiatric findings in Wolfram syndrome homozygotes. Lancet 336, 667–669.

Takeda, K., Inoue, H., Tanizawa, Y., Matsuzaki, Y., Oba, J., Watanabe, Y., Shinoda, K., Oka, Y., 2001. WFS1 (Wolfram syndrome 1) gene product: predominant subcellular localization to endoplasmic reticulum in cultured cells and neuronal expression in rat brain. Hum. Mol. Genet. 10, 477–484.

Takei, D., Ishihara, H., Yamaguchi, S., Yamada, T., Tamura, A., Katagiri, H., Maruyama, Y., Oka, Y., 2006. WFS1 protein modulates the free Ca^{2+} concentration in the endoplasmic reticulum. FEBS Lett. 580, 5635–5640.

Tamamaki, N., Abe, K., Nojyo, Y., 1987. Columnar organization in the subiculum formed by axon branches originating from single CA1 pyramidal neurons in the rat hippocampus. Brain Res. 412, 156–160.

Taube, J.S., Muller, R.U., Ranck Jr., J.B., 1990. Head-direction cells recorded from the postsubiculum in freely moving rats. I. Description and quantitative analysis. J. Neurosci. 10, 420–435.

Tessa, A., Carbone, I., Matteoli, M.C., Bruno, C., Patrono, C., Patera, I.P., De Luca, F., Lorini, R., Santorelli, F.M., 2001. Identification of novel WFS1 mutations in Italian children with Wolfram syndrome. Hum. Mutat. 17, 348–349.

Travers, J.B., 2004. Oromotor nuclei. In: Paxinos, G. (Ed.), The Rat Nervous System. third ed. Elsevier Academic Press, San Diego, pp. 295–319.

Ueda, K., Kawano, J., Takeda, K., Yujiri, T., Tanabe, K., Anno, T., Akiyama, M., Nozaki, J., Yoshinaga, T., Koizumi, A., Shinoda, K., Oka, Y., Tanizawa, Y., 2005. Endoplasmic reticulum stress induces *Wfs1* gene expression in pancreatic β-cells via transcriptional activation. Eur. J. Endocrinol. 153, 167–176.

Van Groen, T., Wyss, J.M., 1990a. The connections of presubiculum and parasubiculum in the rat. Brain Res. 518, 227–243.

Van Groen, T., Wyss, J.M., 1990b. Extrinsic projections from area CA1 of the rat hippocampus: olfactory, cortical, subcortical, and bilateral hippocampal formation projections. J. Comp. Neurol. 302, 515–528.

Van Groen, T., Wyss, J.M., 1990c. The postsubicular cortex in the rat: characterization of the fourth region of the subicular cortex and its connections. Brain Res. 529, 165–177.

Van Groen, T., Wyss, J.M., 1995. Projections from the anterodorsal and anteroventral nucleus of the thalamus to the limbic cortex in the rat. J. Comp. Neurol. 358, 584–604.

van Groen, T., 2001. Entorhinal cortex of the mouse: cytoarchitectonical organization. Hippocampus 11, 397–407.

Vogt, B.A., Miller, M.W., 1983. Cortical connections between rat cingulate cortex and visual, motor, and postsubicular cortices. J. Comp. Neurol. 216, 192–210.

Vogt, B.A., Vogt, L., Farber, N.B., 2004. Cingulate cortex and disease models. In: Paxinos, G. (Ed.), The Rat Nervous System. third ed. Elsevier Academic Press, San Diego, pp. 705–727.

Waite, P.M.E., 2004. Trigeminal sensory system. In: Paxinos, G. (Ed.), The Rat Nervous System. third ed. Elsevier Academic Press, San Diego, pp. 817–851.

Warr, W.B., de Olmos, J.S., Heimer, L., 1981. Horseradish peroxidase: the basic procedure. In: Heimer, L., Robards, M.J. (Eds.), Neuroanatomical Tract-tracing Methods. Plenum Press, New York, pp. 207–262.

Wasson, J., Permutt, M.A., 2008. Candidate gene studies reveal that the *WFS1* gene joins the expanding list of novel type 2 diabetes genes. Diabetologia 51, 391–393.

Witter, M.P., Amaral, D.G., 2004. Hippocampal formation. In: Paxinos, G. (Ed.), The Rat Nervous System. third ed. Elsevier Academic Press, San Diego, pp. 635–704.

Wolfram, D.J., Wagener, H.P., 1938. Diabetes mellitus and simple optic atrophy among siblings: report of four cases. Mayo Clin. Proc. 13, 715–718.

Wouterlood, F.G., 1991. Innervation of entorhinal principal cells by neurons of the nucleus reuniens thalami. Anterograde PHA-L tracing combined with retrograde fluorescent tracing and intracellular injection with Lucifer yellow in the rat. Eur. J. Neurosci. 3, 641–647.

Wouterlood, F.G., Saldana, E., Witter, M.P., 1990. Projection from the nucleus reuniens thalami to the hippocampal region: light and electron microscopic tracing study in the rat with the anterograde tracer Phaseolus vulgaris-leucoagglutinin. J. Comp. Neurol. 296, 179–203.

Woznicka, A., Malinowska, M., Kosmal, A., 2006. Cytoarchitectonic organization of the entorhinal cortex of the canine brain. Brain Res. Rev. 52, 346–367.

Wyss, J.M., Van Groen, T., 1992. Connections between the retrosplenial cortex and the hippocampal formation in the rat: a review. Hippocampus 2, 1–11.

Yamada, T., Ishihara, H., Tamura, A., Takahashi, R., Yamaguchi, S., Takei, D., Tokita, A., Satake, C., Tashiro, F., Katagiri, H., Aburatani, H., Miyazaki, J., Oka, Y., 2006. WFS1-deficiency increases endoplasmic reticulum stress, impairs cell cycle progression and triggers the apoptotic pathway specifically in pancreatic β-cells. Hum. Mol. Genet. 15, 1600–1609.

Yamaguchi, S., Ishihara, H., Tamura, A., Yamada, T., Takahashi, R., Takei, D., Katagiri, H., Oka, Y., 2004. Endoplasmic reticulum stress and N-glycosylation modulate expression of WFS1 protein. Biochem. Biophys. Res. Commun. 325, 250–256.

Young, T.L., Ives, E., Lynch, E., Person, R., Snook, S., MacLaren, L., Cater, T., Griffin, A., Fernandez, B., Lee, M.K., King, M.C., 2001. Non-syndromic progressive hearing loss *DFNA38* is caused by heterozygous missense mutation in the Wolfram syndrome gene *WFS1*. Hum. Mol. Genet. 10, 2509–2514.

Anal Bioanal Chem (2009) 394:1655–1660
DOI 10.1007/s00216-009-2830-9

ORIGINAL PAPER

Pattern recognition analysis for ^{1}H NMR spectra of plasma from hemodialysis patients

Masako Fujiwara · Takeshi Kobayashi · Takahiro Jomori · Yutaka Maruyama · Yoshitomo Oka · Hiroshi Sekino · Yutaka Imai · Kazuhisa Takeuchi

Received: 9 March 2009 / Revised: 28 April 2009 / Accepted: 30 April 2009 / Published online: 1 June 2009

Abstract ^{1}H NMR spectroscopic and pattern recognition-based methods (NMR-PR) were applied to the metabolic profiling studies on hemodialysis (HD). Plasma samples were collected from 37 patients before and after HD and measured by 600 MHz NMR spectroscopy. Each spectrum was data-processed and subjected to principal component analysis for pattern recognition. Spectral patterns of plasma between pre- and post-dialyses were clearly discriminated, together with significant fluctuations in the levels of creatinine, trimethylamine-*N*-oxide, glucose, lactate, and acetate, which were quantitated. We have first observed the significant elevation of lactate levels in post-dialysis plasma. The present study has demonstrated the high feasibility of NMR-PR method for monitoring the dialysis condition and comprehensive profiling of the change of low-molecular-weight metabolites in HD.

Keywords Lactate · Acetate · TMAO · PCA · Renal failure · Metabolomics

M. Fujiwara (✉) · T. Kobayashi · Y. Imai · K. Takeuchi
Graduate School of Pharmaceutical Sciences, Tohoku University,
6-3, Aramaki-aza-aoba, Aoba-ku,
Sendai 980-8578, Japan
e-mail: fmasako@m.tains.tohoku.ac.jp

T. Jomori
Faculty of Pharmaceutical Sciences, Tohoku University,
Sendai, Japan

M. Fujiwara · Y. Maruyama · Y. Imai
The Tohoku University 21st Century COE Program
"CRESCENDO",
Sendai, Japan

Y. Oka
Division of Molecular Metabolism and Diabetes,
Graduate School of Medicine, Tohoku University,
Sendai, Japan

H. Sekino · K. Takeuchi
CKD Center, Koujinkai Central Hemodialysis Clinic,
Sendai, Japan

Present Address:
Y. Maruyama
Department of Career Development, Seiwa Gakuen College,
Sendai, Japan

Introduction

NMR spectroscopy of biofuilds has introduced a new chemistry analysis tool to life science and clinical medicine with the high filed NMR spectrometers [1]. The technique has been applied to various disease characterization and diagnostic or prognostic researches on cardiovascular diseases [2], cancer [3], inborn errors of metabolism [4], diabetes [5, 6], arthritis [7], liver disease [8], etc. [9]. The studies on renal failure [10–13] and HD therapy [14] have been performed as well. The previous metabolomic study using ^{1}H NMR spectroscopy in HD patients under the HD buffer containing acetate showed an accumulation of acetate and metabolism during the course of the dialysis and demonstrated changes in the relative concentrations of endogenous plasma components [15]. A subsequent ^{1}H, ^{13}C, and ^{14}N NMR study of the plasma and urine from renal failure patients showed that the plasma levels of TMAO (trimethylamine-*N*-oxide) correlated with those of urea and creatinine, suggesting that the presence of TMAO is closely related to the degree of renal failure [16]. In these studies, however, the subject number was limited.

NMR metabolomics combined with multivariate pattern recognition would give an advantage over other conventional

analyses. The method of principal component analysis (PCA) simplifies the multivariate data into two or three dimensions that can be readily understood and evaluated [17]. This analysis allows one to discriminate between different subgroups existent in the total population by their characteristic patterns of spectra [18, 19]. It is also possible to identify the relevant biomarkers [20]. PCA does not require any identification of signals but the processed numerical data from spectra intensity (non-targeted analysis) [21]. The score plot can depict classification of groups by the characteristic of spectral patterns [22].

The purpose of our study was to assess the utility of ^{1}H NMR metabolomics using pattern recognition analysis of plasma in HD. In the present study, plasma from 37 patients were measured by ^{1}H NMR spectroscopy and subjected to PCA. The analysis has revealed some metabolites behaviors: elevation of acetate, glucose, and lactate in post-dialysis plasma, of which levels were quantitated by ^{1}H NMR spectroscopy.

Methods

Patients Thirty-seven patients had been studied. After the approval of the study protocol by the ethical committee (Koujinkai Central Hemodialysis Clinic, Sendai, Japan), informed consents have been obtained. The characteristic were age between 39 and 93 years; gender, 48% women; and cause of renal failure, diabetic nephropathy diabetes mellitus 34%, chronic glomerulonephritis or nephropathy 34%, and others (nephrosclerosis, congenital renal disease, etc.). Their hemodialysis conditions were stable, and the duration of hemodialysis was between 2 and 32 years (average, 10.5 years). Their metabolic findings such as levels of blood glucose and lipids were not significantly different in the patients.

Samples Venous blood samples from subjects undergoing HD using bicarbonate dialysis buffers (containing acetate of 8–12 mM and glucose of 5–8 mM) were collected into lithium heparin tubes. After centrifuging, the plasma was stored at −20 °C. It was thawed at room temperature immediately before use, and any precipitation was removed by centrifugation. For NMR, 200 µl of plasma and 400 µl so-called NMR cocktail (saline with 5 mM TSP (sodium 3-(trimethylsilyl) propionic 2, 2, 3, 3-d_4) as both concentration and chemical shift reference, NaN_3 for preventing and D_2O 50 µl for the internal field-frequency lock) was placed into 5-mm NMR tube.

NMR spectroscopy Single-pulse ^{1}H NMR spectra were recorded at 35 °C internal probe temperature using 600 MHz NMR spectrometer (JEOL ECA) quipped with a sample changer. Each spectrum consisted of 64 K complex data points with a spectrum width 6 kHz, where each spectrum was accumulated by 64 scans with an acquisition time of 1.75 s and a recycle delay of 5 s per scan. The detection pulse flip angle was set to 45°. A pre-saturation sequence was used to suppress the water signal.

NMR data reduction procedures Each NMR spectrum was segmented into 225 regions of 0.04 ppm width over the range of 0.5 to 9.5 ppm, and each segment of the spectral regions was integrated. Integrated regions from 4.3 to 5.2 ppm, which contained residual water resonance, were eliminated from the data table, and then data were reduced to 202 variable regions. The remaining integral values of each spectrum were normalized for 100 of the total summed integrals in order to compensate for any differences of the plasma samples. These processing and successive PCA was performed by ALICE2 for Metabolome® software package (version 1.0; JEOL, Tokyo, Japan).

Quantitation of metabolites Serial additions of lactate (0.5, 1.0, 1.5, 2.0, 3.0, and 5.0 mM) were performed to the randomly selected three-paired samples of pre- and post-plasma. Every result of six experiments exhibited the linear relation between the signal area of each addition and the concentration lactate added. The chemical shift and line-width did not change on each experiment. The sensitivity of signal area vs. concentration was not exactly same in each sample. However, six sensitivities revealed to be within ±10% deviation from the average. In the present study, the practical approximation was applied for use of this average sensitivity to calibrate the absolute lactate concentration of signal areas. The values of concentrations for glucose and acetate were calculated in the same way by using corresponding proton numbers [15].

Results

Metabolic profiling by ^{1}H NMR

Figure 1 shows the representative plasma spectra of pre- and post-dialysis using bicarbonate buffer containing acetate and the spectrum of initial waste fluid from dialyser. In Fig. 1a of the pre-dialysis spectrum, the resonances of methyl (3.04 ppm) and methylene (4.05 ppm) of creatinine and methyls (3.28 ppm) of TMAO were significantly increased comparative with that of post-dialysis in which acetate (1.92 ppm) signal appeared [23]. Glucose exhibited many sharp signals between creatinine peaks in both spectra in Fig. 1a and b. Every pre-dialysis spectrum had little signal of acetate. The waste solution measured was taken 15 min after the start of dialysis treatment, and the spectrum exhibited not only signals of acetate and glucose

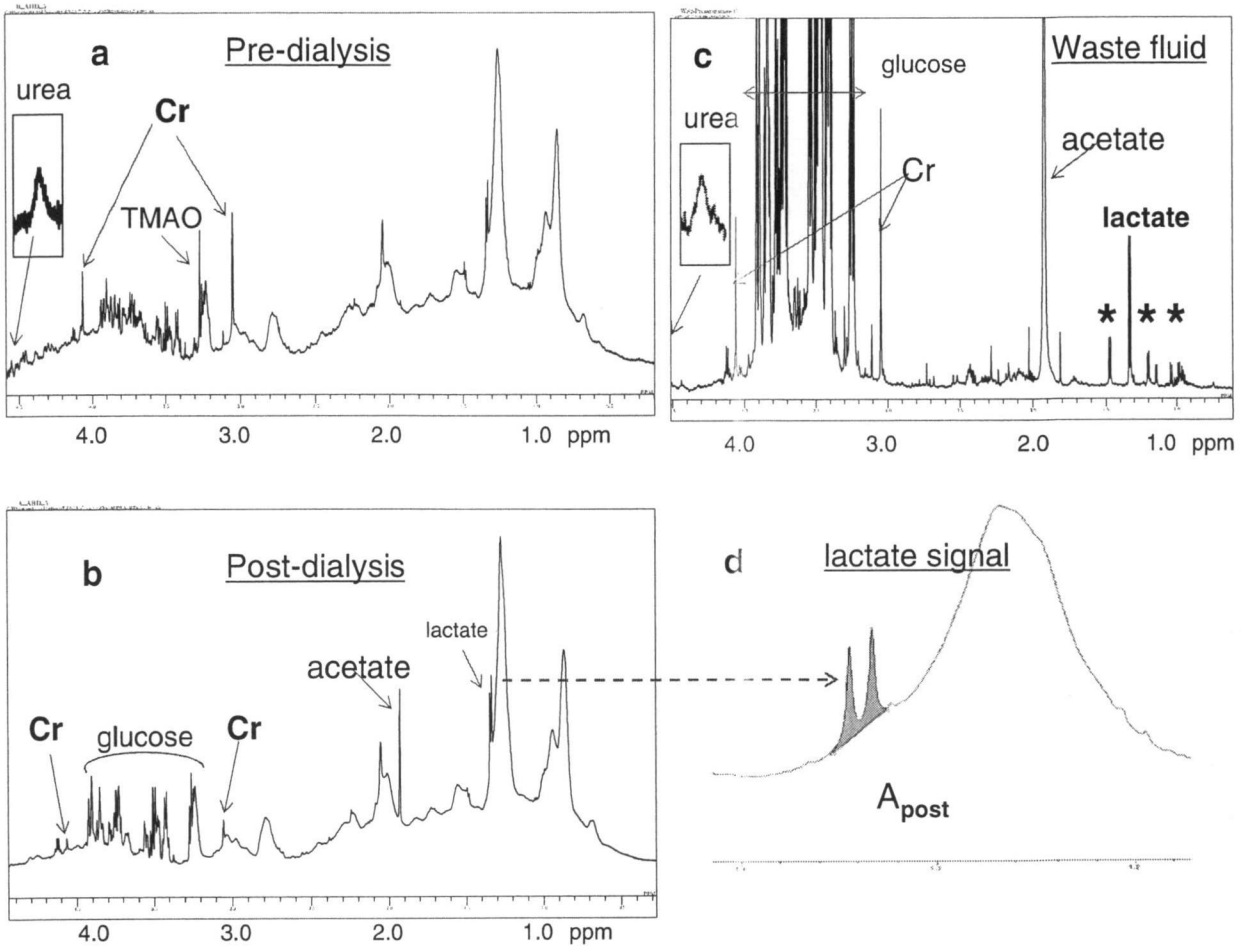

Fig. 1 ^{1}H NMR spectra (600 MHz) of plasma from pre- and post-dialysis (**a**, **b**) and of waste fluid (**c**) in the higher field, respectively. Cr indicates creatinine signal. In each spectra (**a**, **c**), there was a signal of urea at 5.78 ppm inserted to the figure with enlargement, respectively. In **c**, the *asterisk-marked* signals indicate valine, threonine, and alanine from the right, respectively. **d** The enlargement of lactate signal. The signal areas, A_{post} and A_{pre}, were measured after adequate baseline correction indicated as a *shaded area*, respectively, and used for calculation of Δ

in dialysate fluid constituents but also those of creatinine, lactate, amino acids, and organic acids that were filtered out of plasma already.

^{1}H NMR spectra of 37 pairs (pre- and post-dialysis plasma) were measured and processed as mentioned above and submitted to PCA. As shown in Fig. 2a, the two groups were clearly separated. The PC1 axis successfully extracted dialysis effect dominantly. Loading plot is shown in Fig. 2b; the distribution of variables corresponds to that of samples in score plot. The lower group reflects the increase level of acetate; samples of right side have larger signals of lipid so on. Figure 2c shows distribution of contribution of variables to PCs; every bar (variable) consists of contributions to PC1 (red), PC2 (blue), PC3 (green), and the residuals (cyan). The variables of lipid and glucose in Fig. 2c have large contribution to PC2, which corresponds to PC2, i.e., the horizontal axis of score plot in Fig. 2a. The variable of 3.28 ppm (TMAO) has the big contribution to PC3 nearly the same ratio as that to PC1.

Figure 2d showed also the loading depicted in the cross-sectional graph of Fig. 2b along PC1 axis. This profile of all the metabolites was responsible for making PC1 axis to characterize and discriminate the two groups. The upper bars, including creatinine, TMAO, threonine, alanine, etc., are large in the upper group samples (pre-), and the lower bars, including glucose, acetate, and lactate, are large in the lower group samples (post-) in Fig. 2a, respectively. This figure illustrates the quantitative fluctuation of all the metabolites simultaneously. The lower big bar of acetate and glucose were considered to be derived from dialysis fluid constituents; however, elevated post-plasma level of lactate was unexpectedly observed.

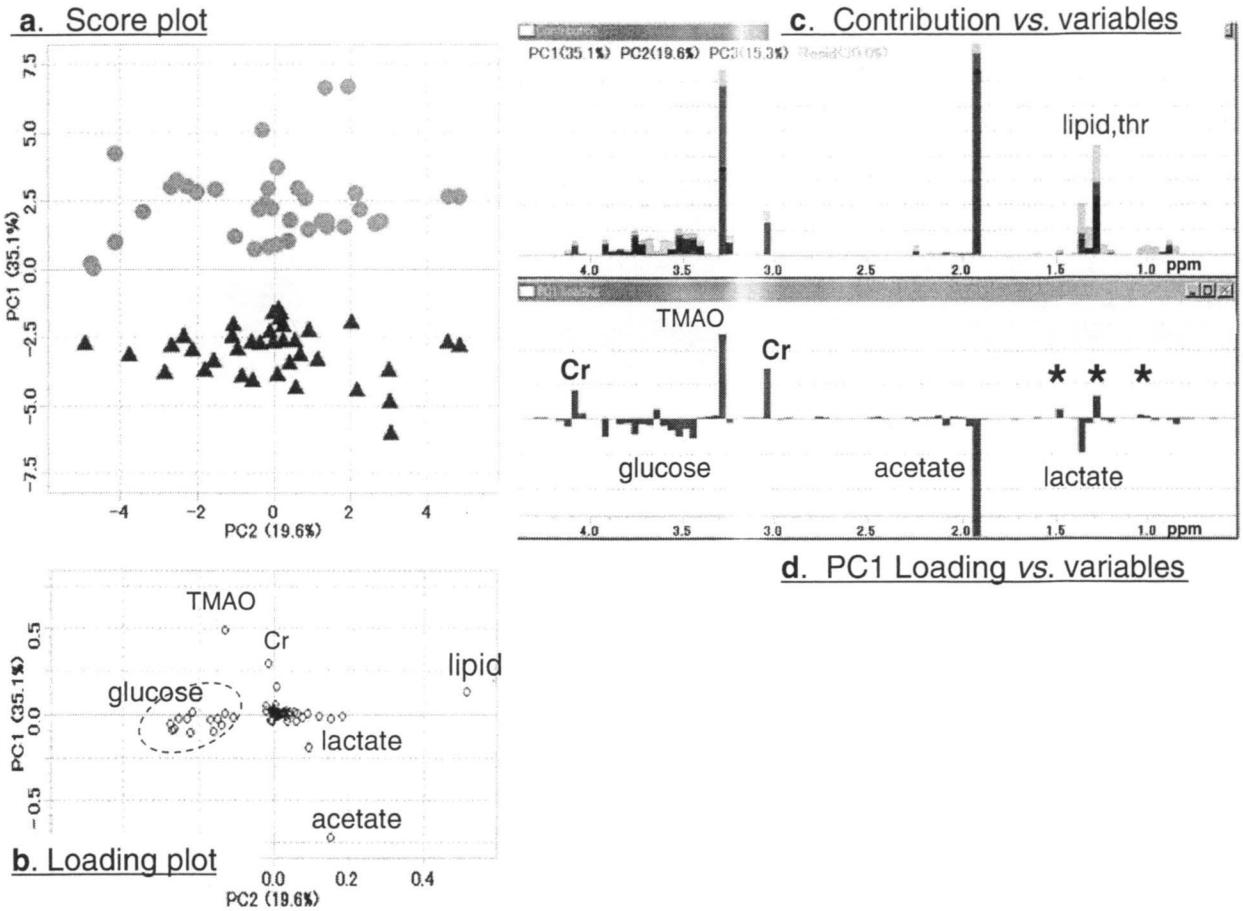

Fig. 2 **a** PCA score plot of PC1-PC2; *orange circle* and *purple triangle dots* indicate spectra from pre- and post-dialysis subjects, respectively. PC1 and PC2 explained 31.5% and 19.8% of total variance, respectively. **b** Loading plot; major metabolites were indicated. **c** Contribution quantities of variables in higher field showing that responsible for PCA classification. The *red*, *blue*, *green*, and *cyan bars* correspond to the contribution to PC1, PC2, PC3, and the residuals, respectively. **d** A plot of PC1 loading vs. variables. The *asterisk-marked* variables are valine, threonine, and alanine corresponding to Fig. 1

Quantitation of creatinine, TMAO, acetate, glucose, and lactate

For further investigation, we tried to quantify metabolites that changed greatly, creatinine, TMAO, acetate, glucose, and lactate, between pre- and post-treatment.

We have quantitated by integration of signal areas from small metabolites [24] after adequate baseline correction like as in Fig. 1d. For the quantitation of differences between pre- and post-resonances of the metabolites, the subtraction pre-signal area A_{pre} from post-signal area A_{post}, that is, $\Delta = A_{post} - A_{pre}$, was calculated for each paired

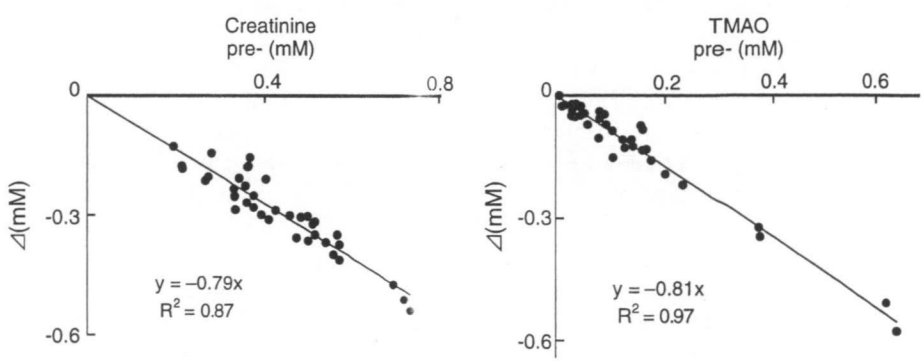

Fig. 3 Correlation of the concentration between pre- and difference of 37 subjects in mM, respectively. A *red line* indicates 0 value of Δ on each graph. Linear regression line was depicted on graphs of creatinine and TAMO

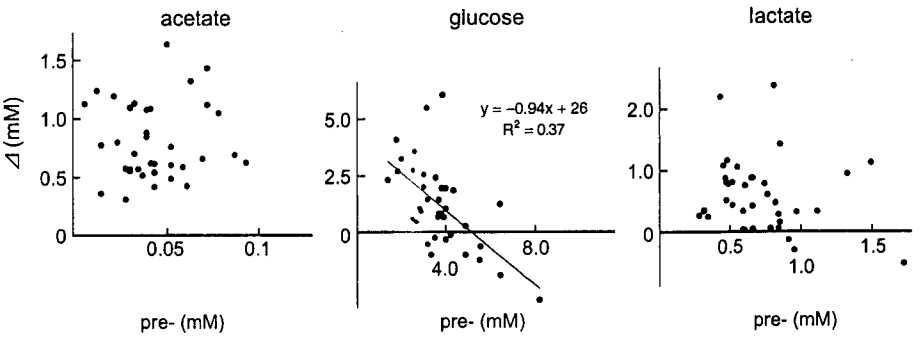

Fig. 4 Correlations of concentration between pre- and difference of 37 subjects for acetate, glucose, and lactate, in mM, respectively. A *red line* indicates 0 value of Δ on each graph

spectra. We determined graded several concentrations of lactate added to samples for the transformation signal areas to concentration, as mentioned in the previous section. Thus, the concentrations of pre-dialysis vs. the difference (Δ) for metabolites of 37 were plotted in mM in Figs. 3 and 4.

In Fig. 3, differences of creatinine and TMAO were revealed to have all negative values, which show successful clearance by dialysis, and to be greatly dependent upon the initial accumulated values of each. The linear regression graphs showed the following relation,

$$\Delta = A_{post} - A_{pre} \fallingdotseq -0.8\, A_{pre}$$

Then $A_{post} \fallingdotseq 0.2\, A_{pre}$

Values of post- became 1/5 that of pre-; it meant the treatment cleared 80% of accumulated ureic toxins.

As shown in Fig. 4, the differences (Δ) of acetate showed all positive values with much variance, that of glucose presented mostly positive values with a negative correlation to its pre- values, and the most values of that for lactate were significantly positive with much variance. These concentrations of average and maximum of all 37 samples were summarized in Table 1.

Discussion

NMR method requires little or no pretreatment of the sample, and it allows a simultaneous quantitation of metabolites in a spectrum [15]. NMR-PR method has no specific target metabolites to be analyzed but it reveals whole spectral pattern, and therefore, the statistical analysis of PCA leads to comprehensive profile, including not only creatinine, TMAO, glucose, and acetate but also lactate and others. The present analysis clearly extracted the balance change.

We have showed that creatinine, TMAO, alanine, thereonine, and other low-molecule metabolites were cleared from plasma by dialysis, while acetate, glucose, and lactate levels were elevated in post-dialysis plasma. TMAO accumulation in the end-stage-kidney disease [16] and its clearance by dialysis have already been reported [25]. We here observed a weak correlation between pre-dialysis plasma levels of TMAO and creatinine, although the levels of TMAO vary, probably depending on the amount of dietary intake which digest TMAO, such as fish meat [24]. The dialysate constituents could cause acetate level increment, as expected. The variance of Δ acetate values shown in Fig. 4 was due to individual variety. As for glucose, the values were varied probably due to the balance between the plasma levels of glucose and dialysis buffer or the meal intake during HD

In the post-HD, plasma levels of lactate were significantly increased. There has been no report on the observation. As shown in Fig.1c, lactate is a small molecule to be filtered continuously with the same ratio as creatinine and TMAO; the increment plasma level of lactate (its average of 0.7 mM as shown in Table 1) was due to a de novo synthesis during HD. The cause of lactate increase is unknown. In HD, dehydration would lower blood perfusion to tissues, leading to the peripheral hypoxemia resulting in anaerobic glycolysis causing lactate synthesis, or the change of pH during HD may influence the degradation of lactate by lactate dehydrogenase [26].

In conclusion, NMR-PR method has promising scope for a monitoring HD treatment together with comprehensive and visual metabolic profiling.

Table 1 The values of mean and maximum of 37 samples (mM)

		mean±SD	max
lactate	pre	0.9±0.4	2.1
	post	1.6±0.6	3.9
	Δ	0.7±0.6	1.8
glucose	pre	3.6±1.4	7.9
	post	4.9±1.6	10.5
	Δ	1.3±2.0	6.6
acetate	pre	0.04±0.02	0.1
	post	0.9±0.3	1.7
	Δ	0.8±0.3	1.6

Acknowledgment This work was supported in part by Grants-in-Aid from the Ministry of Education, Culture, Sports, Science and Technology of Japan (19590930, 20659004) and a grant from Kirin Pharm. Co. Ltd.

References

1. Nicholson JK, Wilson ID (1989) High resolution proton magnetic resonance spectroscopy of biological fluids. Prog Nucl Magn Reson Spectrosc 21:449–551
2. Brindle JT, Antti H, Holmes E, Tranter G, Nicholson JK, Bethell HW, Clarke S, Schofield PM, McKilligin E, Mosedale DE, Grainger DJ (2002) Rapid and noninvasive diagnosis of the presence and severity of coronary heart disease using ^{1}H NMR-based metabolomics. Nat Med 8:1430–1444
3. Chen LL, Burns MA, Taylor JL, HE W, Halpern EF, McDougal WS, Wu CL (2005) Metabolic characterization of human prostate cancer with tissue magnetic resonance spectroscopy. Cancer Res 65:3030–3034
4. Moonlenaar SH, Engelke UF, Wevers RA (2003) Proton nuclear magnetic resonance spectroscopy of body fluids in the field of inborn errors of metabolism. Ann Clin Biochem 40:16–24
5. Nicholson JK, O'Flynn MP, Sadler PJ, Macleod AF, Juul SM (1984) Proton-nuclear-magnetic-resonance studies of serum, plasma, and urine from fasting normal and diabetic subjects. Biochem J 217:365–375
6. Makinen V-P, Soininen P, Forsblom C, Parkonen M, Ingman P, Kaski K, Groop P-H, Ala-Korpela M (2008) ^{1}H NMR metabonomics approach to disease continuum of diabetic complications and premature death. Mol Syst Biol 4:1–11
7. Parkers HG, Grootveld M, Henderson EB, Farrell A, Blake DR (1991) Oxidative damage to synovial fluid from the inflamed rheumatoid joint detected by ^{1}H NMR spectroscopy. J Pharm Biomed Anal 9:75–82
8. Clayton TA, Lindon JC, Everett JR, Charuel C, Hanton G, Net LJ-L, Provost J-P, Nicholson JK (2004) Hepatotoxin-induced hypercreatinaemia and hypercreatinuria: their relationship to one another, to liver damage and to weakened nutritional status. Arch Toxicol 78:86–96
9. Lindon JC, Holmes E (2007) A survey of metabolomics approaches for disease characterization. In: Lindon JC et al (ed) The handbook of metabonomics and metabolomics. Elsevier B. V., Amsterdam, pp. 427–434
10. Knubovets TL, Lundina TA, Sibeldina LA, Sedov KR (1992) ^{1}H NMR urinalysis in glomerulopheritis: a new prognostic criterion. Magn Reson Imaging 10:127–134
11. Holmes E, Foxall PJD, Nicholson JK (1990) Proton NMR analysis of plasma from renal failure patients: Evaluation of sample preparation and spectral-editing method. J Pharm Biomed Anal 8:955–958
12. Foxall PJD, Spraul M, Farrant RD, Lindon JC, Nicholson JK (1993) 750 MHz ^{1}H NMR spectroscopy of human blood plasma. J Pharm Biomed Anal 11:267–276
13. Foxall PJD, Price RG, Jones JK, Neild GH, Tompson FD, Nicholson JK (1992) High resolution proton magnetic resonance spectroscopy of cyst fluid from patients with polycystic kidney disease. Biochem Biophys Acta 1138:305–314
14. Scholze A, Jankowski V, Henning L, Haass W, Wittstock A, Suvd-Erdene S, Zidek W, Tepel M, Jankowski J (2007) Phenylacetic acid and arterial vascular properties in patients with chronic kidney disease stage 5 on hemodialysis therapy. Nephron Clin Pract 107:1–6
15. Grasdalen H, Belton PS, Pryor JA, Rich GT (1987) Quantitative proton magnetic resonance of plasma from uraemic patients during dialysis. Magn Reson Chem 25:811–816
16. Bell JD, Lee A, Lee HA, Sadler PJ, Wdkle DR, Woodhaml RH (1991) Nuclear magnetic resonance studies of blood plasma and urine from subjects with chronic renal failure: identification of trimethylamine-N-oxide. Biochemica et Biophysica Acta 1096:101–107
17. Xu L (ed) (1995) Methods of chemometrics. Science, Beijing
18. Holmes E, Nicholls AW, Lindon JC, Ramos S, Spraul M, Neidig P, Connor SC, Connelly J, Damment SJP, Haselden J, Nicholson JK (1998) Developing of a model for classification of toxin-induced lesions using ^{1}H NMR spectroscopy of urine combined with pattern recognition. NMR Biomed 11:235–244
19. Fujiwara M, Ando I, Arifuku K, Nemoto T (2005) Pattern recognition analysis for classification of hypertensive model rats and diurnal variation using ^{1}H-NMR spectroscopy of urine. Anal Sci 21:1259–1262
20. Duarte IF, Goodfellow BJ, Barros A, Jones JG, Barosa C, Diogo L, Garcia P, Gil AM (2007) Metabolic characterization of plasma in juveniles with glycogen storage disease type 1a (GSD1a) by high-resolution ^{1}H NMR spectroscopy. NMR Biomed 20:401–412
21. Nemoto T, Ando I, Kataoka T, Arifuku K, Kanazawa K, Natori Y, Fujiwara M (2007) NMR metabolic profiling combined with two-step principal component analysis for toxin-induced diabetes model rat using urine. J Toxicol Sci 32:429–435
22. Maher AD, Zirah SFM, Holmes E, Nicholson JK (2007) Experimental and analytical variation in human urine in ^{1}H NMR spectroscopy-based metabolic phenotyping studies. Anal Chem 79:5204–5211
23. Nicholson JK, Foxall PJD (1995) 750 MHz ^{1}H and ^{1}H–^{13}C NMR spectroscopy of human blood plasma. Anal Chem 67:793–811
24. Mascre S, Wahl A, Azaroual N, Boulet O, Crunelle V, Imbenotte M, Lhard M, Vemeersch G, Lhermitte M (1997) ^{1}H NMR analysis of trimethylamine in urine for the diagnosis of fish-odour syndrome. Clin Chim Acta 263:139–146
25. Bain MA, Faull R, Fornasini G, Milne RE, Evans AM (2006) Accumulation of trimethylamine and trimethylamine-*N*-oxide in end-stage renal disease patients undergoing haemodialysis. Nephrol Dial Transplant 21:1300–1304
26. Bellomo R (2002) Bench-to-bedside review: lactate and the kidney. Crit Care 6:322–326

Journal of Human Genetics (2009) 54, 236–241

www.nature.com/jhg

ORIGINAL ARTICLE

Construction of a prediction model for type 2 diabetes mellitus in the Japanese population based on 11 genes with strong evidence of the association

Kazuaki Miyake[1], Woosung Yang[2], Kazuo Hara[3], Kazuki Yasuda[4], Yukio Horikawa[5], Haruhiko Osawa[6], Hiroto Furuta[7], Maggie CY Ng[8], Yushi Hirota[1], Hiroyuki Mori[1], Keisuke Ido[2,20], Kazuya Yamagata[9,21], Yoshinori Hinokio[10], Yoshitomo Oka[10], Naoko Iwasaki[11], Yasuhiko Iwamoto[11], Yuichiro Yamada[12,22], Yutaka Seino[12,23], Hiroshi Maegawa[13], Atsunori Kashiwagi[13], He-yao Wang[4,24], Toshihito Tanahashi[14], Naoto Nakamura[15], Jun Takeda[5], Eiichi Maeda[2], Ken Yamamoto[16], Katsushi Tokunaga[17], Ronald CW Ma[8], Wing-Yee So[8], Juliana CN Chan[8], Naoyuki Kamatani[18], Hideichi Makino[6], Kishio Nanjo[7], Takashi Kadowaki[3] and Masato Kasuga[1,19]

Prediction of the disease status is one of the most important objectives of genetic studies. To select the genes with strong evidence of the association with type 2 diabetes mellitus, we validated the associations of the seven candidate loci extracted in our earlier study by genotyping the samples in two independent sample panels. However, except for *KCNQ1*, the association of none of the remaining seven loci was replicated. We then selected 11 genes, *KCNQ1*, *TCF7L2*, *CDKAL1*, *CDKN2A/B*, *IGF2BP2*, *SLC30A8*, *HHEX*, *GCKR*, *HNF1B*, *KCNJ11* and *PPARG*, whose associations with diabetes have already been reported and replicated either in the literature or in this study in the Japanese population. As no evidence of the gene–gene interaction for any pair of the 11 loci was shown, we constructed a prediction model for the disease using the logistic regression analysis by incorporating the number of the risk alleles for the 11 genes, as well as age, sex and body mass index as independent variables. Cumulative risk assessment showed that the addition of one risk allele resulted in an average increase in the odds for the disease of 1.29 (95% CI=1.25–1.33, $P=5.4\times10^{-53}$). The area under the receiver operating characteristic curve, an estimate of the power of the prediction model, was 0.72, thereby indicating that our prediction model for type 2 diabetes may not be so useful but has some value. Incorporation of data from additional risk loci is most likely to increase the predictive power.
Journal of Human Genetics (2009) **54**, 236–241; doi:10.1038/jhg.2009.17; published online 27 February 2009

Keywords: gene–gene interaction; genome-wide association study; prediction model; single nucleotide polymorphism (SNP); type 2 diabetes mellitus

[1]Division of Diabetes, Metabolism and Endocrinology, Department of Internal Medicine, Kobe University Graduate School of Medicine, Kobe, Japan; [2]Clinical Genome Informatics Center, Kobe University Graduate School of Medicine, Kobe, Japan; [3]Department of Metabolic Diseases, Graduate School of Medicine, University of Tokyo, Tokyo, Japan; [4]Department of Metabolic Disorder, Research Institute, International Medical Center of Japan, Tokyo, Japan; [5]Division of Molecule and Structure, Department of Diabetes and Endocrinology, Gifu University School of Medicine, Gifu, Japan; [6]Department of Molecular and Genetic Medicine, Ehime University Graduate School of Medicine, Ehime, Japan; [7]First Department of Medicine, Wakayama Medical University, Wakayama, Japan; [8]Department of Medicine and Therapeutics, The Chinese University of Hong Kong, Shatin, Hong Kong; [9]Department of Metabolic Medicine, Graduate School of Medicine, Osaka University, Osaka, Japan; [10]Division of Molecular Metabolism and Diabetes, Tohoku University Graduate School of Medicine, Sendai, Japan; [11]Department of Medicine, Diabetes Center, Tokyo Women's Medical University, Tokyo, Japan; [12]Department of Diabetes and Clinical Nutrition, Kyoto University School of Medicine, Kyoto, Japan; [13]Division of Endocrinology and Metabolism, Department of Medicine, Shiga University of Medical Science, Shiga, Japan; [14]Division of Genetic Information, Institute for Genome Research, University of Tokushima, Tokushima, Japan; [15]Department of Endocrinology and Metabolism, Kyoto Prefectural University of Medicine, Graduate School of Medical Sciences, Kyoto, Japan; [16]Department of Molecular Genetics, Medical Institute of Bioregulation, Kyushu University, Fukuoka, Japan; [17]Department of Human Genetics, Graduate School of Medicine, University of Tokyo, Tokyo, Japan; [18]Division of Genomic Medicine, Department of Advanced Biomedical Engineering and Science, Tokyo Women's Medical University, Tokyo, Japan and [19]Research Institute, International Medical Center of Japan, Tokyo, Japan

Correspondence: Dr M Kasuga, Research Institute, International Medical Center of Japan, 1-21-1 Toyama, Shinjuku-ku, Tokyo 162-8655, Japan.
E-mail: kasuga@ri.imcj.go.jp

[20]Current address: Information Center for Medical Sciences, Tokyo Medical and Dental University, Tokyo, Japan.
[21]Current address: Faculty of Medical and Pharmaceutical Sciences, Department of Medical Biochemistry, Kumamoto University, Kumamoto, Japan.
[22]Current address: Department of Internal Medicine, Akita University School of Medicine, Akita, Japan.
[23]Current address: Kansai Electric Power Hospital, Osaka, Japan.
[24]Current address: Shanghai Institute of Materia Medica, Chinese Academy of Science, Shanghai, China.
Received 22 December 2008; revised 25 January 2009; accepted 5 February 2009; published online 27 February 2009

INTRODUCTION

Genome-wide association studies (GWASs) have identified novel susceptibility genes for type 2 diabetes mellitus in Caucasians.[1–5] *TCF7L2*, *CDKAL1*, *CDKN2A/B*, *IGF2BP2*, *SLC30A8* and *HHEX* have been widely replicated as susceptibility genes for type 2 diabetes in Asian populations[6–12] as well as in populations of European ancestry.[13,14] We recently identified *KCNQ1* as a novel susceptibility gene, as well as seven other candidate susceptibility loci in a multistage GWAS for type 2 diabetes in the Japanese population, in which a total of 1612 cases and 1424 controls and 100 000 single nucleotide polymorphisms (SNPs) were included.[15] *KCNQ1* was found to confer risk of type 2 diabetes with a relatively large effect size in Asian populations (odds ratio (OR) for Japanese, Chinese and Korean individuals of 1.42),[15] which was similar to that demonstrated earlier for *TCF7L2* in the Japanese population.[6]

Follow-up of GWASs includes analysis of second-tier genes, meta-analysis for specific populations, as well as analysis of gene–gene or gene–environment interactions. A large-scale meta-analysis[16] and an analysis of gene–gene interaction for susceptibility genes[17] have been performed for type 2 diabetes in populations of European ancestry.

In this study, we attempted to confirm in independent subject panels of Japanese and Hong Kong Chinese individuals the associations of the seven candidate susceptibility loci that we identified in addition to *KCNQ1* in our GWAS of type 2 diabetes.[15] However, as described in this article, we failed to replicate the associations of the seven loci with diabetes. We then attempted to extract genes with strong evidence of the associations with diabetes, and selected 11 genes, including *KCNQ1*. As we did not detect any gene–gene interaction between the 11 genes, we then attempted to construct a prediction model for this disease by using the data from the 11 genes, as well as age, gender and body mass index (BMI) as independent variables to obtain a comprehensive understanding of the genetic background of diabetes in the Japanese population.

MATERIALS AND METHODS

Validation of the results from a multistage GWAS in the Japanese population

Study subjects. We assembled two independent subject panels for our replication study: replication-Japanese and replication-Chinese. The 1000 cases and 1000 controls for the replication-Japanese panel were recruited by the Study Group of the Millennium Genome Project for Diabetes Mellitus. The inclusion criteria for diabetic patients were (i) an age at disease onset of 30–60 years and (ii) the absence of antibodies to GAD. Types of diabetes other than type 2 were excluded on the basis of clinical data. The criteria for controls included (i) an age of >50 years, (ii) no past history of a diagnosis of diabetes and (iii) an HbA_{1c} content of <5.8%.

For the replication-Chinese panel, subjects of southern Han Chinese ancestry, who resided in Hong Kong, were recruited. The cases consisted of 1416 individuals with type 2 diabetes selected from the Prince of Wales Hospital Diabetes Registry;[5,18] 626 of these subjects had early-onset diabetes (age at diagnosis of <40 years) and a positive family history, whereas the remaining 790 patients were randomly selected from the registry. Patients with classic type 1 diabetes with acute ketotic presentation or a continuous requirement for insulin within 1 year of diagnosis were excluded. The controls consisted of 1577 subjects with normal glucose tolerance (fasting plasma glucose concentration of <6.1 mmol l^{-1}); 596 of these individuals were recruited either from the general population participating in a community-based screening program for cardiovascular risk or from hospital staff, whereas the remaining 981 subjects were recruited from a population-based screening program for cardiovascular risk in adolescents.[19] The clinical characteristics of the subjects in each panel are summarized in Supplementary Table 1A. The study protocol was approved by the local ethics committee of each institution. Written informed consent was obtained from each subject.

Study design and statistical analysis. For the validation of the results from our earlier multistage GWAS,[15] seven SNPs (rs2250402, rs2307027, rs3741872, rs574628, rs2233647, rs3785233 and rs2075931) were genotyped in the two panels either by sequence-specific primer–PCR analysis followed by fluorescence correlation spectroscopy[20] or by real-time PCR analysis with TaqMan probes (Applied Biosystems, Foster City, CA, USA). Differences in allele frequency between cases and controls for each SNP were evaluated by χ^2 with one degree of freedom. Meta-analysis was performed by the Mantel–Haenszel method (fixed-effects models) with the 'meta' package of the R-Project (http://www.r-project.org). A *P*-value of <0.05 was considered statistically significant.

Examination of gene–gene interaction and construction of a prediction model

Study subjects. In total, 2424 cases and 2424 controls of the Japanese population obtained by combining the second and third screening panels in our original study[15] and the replication-Japanese panel of this study were included in this analysis (analysis-panel). The criteria for the second and third screening panels were described in the earlier report.[15] The clinical characteristics of the subjects are summarized in Supplementary Table 1B.

Selection of the loci included in this study. Prediction of the phenotypes on the basis of genetic polymorphisms should include the genetic data from the loci with strong evidence of the association. Starting from 15 genes described in earlier reports, we selected 11 genes with strong evidence of the association on the basis of the data in the literature and on the results of the replication experiments in this study. Process of the selection of the 11 genes will be described in detail in Results.

Statistical methods. Multiplicative gene–gene interaction was evaluated for each pair of the 11 genes using an interaction term in addition to the terms for the pair of the genes in the logistic regression model. The genotypes for each locus were coded by 0, 1 and 2. Correction for multiple testing was performed by Bonferroni's method.

As there was no evidence for the presence of gene–gene interactions, we attempted to construct a phenotype prediction model by incorporating the number of risk alleles for the 11 loci as an independent variable in addition to age, gender and BMI. The Cochran–Armitage test was used to examine the trend of the increase in the odds by increasing the number of the risk alleles. To construct a prediction model, the log of odds was expressed by the linear combination of the independent variables. Coefficients for the variables were estimated by the logistic regression analysis after making disease (cases) or nondisease (controls) as the dependent variable. Using the coefficients estimated by the logistic regression analysis, we constructed a phenotype prediction model. To evaluate the prediction model, receiver operating characteristic (ROC) curves[21] for the sensitivity and specificity of the prediction model with or without adjustment for age, sex and BMI were generated, and the area under the curve (AUC) was calculated from the ROC curve.

RESULTS

Validation of the results from a multistage GWAS in the Japanese population

We identified earlier 10 loci associated with type 2 diabetes by three-staged GWAS starting from 100 000 SNPs. Among the 10 loci, 3 SNPs were located in an intron of *KCNQ1*, and the association of this gene with diabetes was confirmatory.[15] To validate the other seven loci for the association with type 2 diabetes, we analyzed them in two independent replication panels of Japanese and Han-Chinese individuals (Table 1, Supplementary Table 2). Only one SNP, rs2250402, which is located in *EIF2AK4*, was found to be significantly associated in the replication-Japanese panel (*P*=0.039, OR=1.17, 95% CI=1.01–1.36). However, neither this SNP (*P*=0.41, OR=1.05) nor any of the other six SNPs showed such an association in the replication-Chinese panel. Meta-analyses for these SNPs showed that rs2307027 in *KRT4* and rs3785233 in *A2BP1* yielded *P*-values of <0.05 and ORs between 1.12 and 1.13 (Table 1). When the original second and third screening

Table 1 Association study for the candidate susceptibility genes for type 2 diabetes selected by multistage screening in the Japanese population

SNP ID	*Chr*	*Gene*	*Risk allele*	*Panel*	*RAF (DM)*	*RAF (NC)*	*P*	*OR*	*95% CI*
rs2250402	15	*EIF2AK4*	C	Replication-Japanese	0.23	0.20	0.04	1.17	1.01–1.36
				Replication-Chinese	0.24	0.23	0.41	1.05	0.93–1.19
				Meta-analysis			0.05	1.10	1.00–1.20
rs2307027	12	*KRT4*	C	Replication-Japanese	0.18	0.17	0.17	1.12	0.95–1.32
				Replication-Chinese	0.14	0.13	0.16	1.11	0.96–1.29
				Meta-analysis			0.05	1.12	1.00–1.25
rs3741872	12	*FAM60A*	C	Replication-Japanese	0.25	0.24	0.18	1.11	0.96–1.28
				Replication-Chinese	0.23	0.22	0.21	1.08	0.96–1.22
				Meta-analysis			0.07	1.09	0.99–1.20
rs574628	20	*ANGPT4*	G	Replication-Japanese	0.60	0.61	0.46	0.95	0.84–1.08
				Replication-Chinese	0.65	0.65	0.59	1.03	0.93–1.15
				Meta-analysis			0.96	1.00	0.92–1.08
rs2233647	6	*SPDEF*	G	Replication-Japanese	0.86	0.87	0.70	0.97	0.81–1.16
				Replication-Chinese	0.94	0.93	0.54	1.07	0.87–1.31
				Meta-analysis			0.90	1.01	0.88–1.16
rs3785233	16	*A2BP1*	C	Replication-Japanese	0.18	0.16	0.19	1.12	0.95–1.32
				Replication-Chinese	0.13	0.12	0.10	1.14	0.97–1.34
				Meta-analysis			0.04	1.13	1.01–1.27
rs2075931	1	Intergenic	A	Replication-Japanese	0.67	0.66	0.85	1.01	0.89–1.16
				Replication-Chinese	0.73	0.74	0.27	0.94	0.84–1.05
				Meta-analysis			0.48	0.97	0.89–1.06

Abbreviations: Chr, chromosome; OR, odds ratio for risk allele frequency.
Assignment of risk alleles was based on the original study.[15] Numbers of cases versus control subjects in the replication-Japanese and replication-Chinese panels were 1000 versus 1000 and 1416 versus 1577, respectively. RAF (DM) and RAF (NC) denote risk allele frequencies in cases and controls, respectively. *P* values were calculated for allele frequency. Meta-analysis was performed by the Mantel–Haenszel method (fixed-effects models). *P*-values for the test of heterogeneity among panels joined in the Mantel–Haenszel tests were all >0.05.

panels were included in the meta-analyses, these two loci, as well as the SNPs in *EIF2AK4* (rs2250402) and *FAM60A* (rs3741872), gave *P*-values of <0.001 and ORs between 1.15 and 1.18 (Supplementary Table 3). However, the *P*-values did not reach the proposed significance of GWAS ($=5\times10^{-7}$).

Selection of polymorphisms for the prediction model

To construct a reliable prediction model for diabetes, polymorphisms with strong evidence of association should be used. From the previous literature, we selected 15 genes (including one intergenic marker), that is, *SLC30A8*, *HHEX*, *LOC387761*, *EXT2*, *CDKN2A/B*, *GCKR*, *IGF2BP2*, *CDKAL1*, *FTO*,[1–5] *TCF7L2*,[22] *KCNJ11*,[23] *PPARG*,[24] *WFS1*,[25] *HNF1B*[26] and *KCNQ1*,[15] as candidate genes to be included in both gene–gene interaction analysis and construction of a prediction model. Starting from 23 SNPs in these 15 genes, we selected 11 SNPs in 11 genes according to the following process. There is sufficient evidence of the associations of *KCNQ1* and *TCF7L2* genes with diabetes as supported by replication studies in the Japanese population.[6,15,27] In addition, *SLC30A8*, *HHEX*, *CDKN2A/B*, *IGF2BP2* and *CDKAL1* associated with the disease in the European population were found in our earlier study to be associated with the disease in the Japanese population as well.[7–9]

To further extract genes with strong evidence of the association with diabetes, we attempted to replicate the associations reported earlier using our own data (analysis panel with 2424 cases and 2424 controls). For the 19 SNPs in *SLC30A8*, *HHEX*, *LOC387761*, *EXT2*, *CDKN2A/B*, *GCKR*, *IGF2BP2*, *CDKAL1*, *FTO*, *TCF7L2*, *KCNJ11*, *PPARG* and *KCNQ1*, we extracted genotyping data from our earlier studies[6–9,15,27–29] and, if necessary, genotyped additional subjects to obtain a data set for 2424 cases and 2424 controls of the Japanese population (analysis panel). The SNPs in *WFS1* (rs6446482, rs734312) and *HNF1B* (rs7501939, rs4430796) were genotyped for this study in the same individuals. SNPs with *P*-values for the test of deviation from the Hardy–Weinberg equilibrium of <0.01 were excluded for further analysis. When two SNPs were located in the same genomic region, the one with the lower *P*-value for the association test was selected for further analysis. *GCKR*, for which we earlier reported the marginal association with type 2 diabetes,[7] was found to be associated with the disease in this enlarged Japanese panel ($P=1.7\times10^{-5}$; Supplementary Table 4). *KCNJ11* and *PPARG*, which have been included in the genes associated with diabetes in Caucasians, showed marginal associations ($P=0.066$ and $P=0.075$, respectively; Supplementary Table 4) in our panel. Two SNPs in *WFS1* and two SNPs in *HNF1B* were newly genotyped in the analysis panel. Although no association was apparent between *WFS1* and type 2 diabetes, both SNPs in *HNF1B* exhibited *P*-values of <0.05 (Supplementary Table 4). From these data, we included 11 SNPs in 11 genes as described above for the source of genotype data to be analyzed in both the examination of gene–gene interaction and the prediction of phenotypes.

Gene–gene interaction

We evaluated multiplicative gene–gene interaction for each pair of the 11 loci as described in Materials and methods. Two combinations, rs1801282 (*PPARG*) ×rs1470579 (*IGF2BP2*) (nominal $P=0.0025$) and rs1801282×rs3802177 (*SLC30A8*) (nominal $P=0.018$), showed *P*-values of less than 0.05 (Supplementary Figure 1). However, these *P*-values were not significant when Bonferroni's correction for multiple testing was applied (significance level, $0.05/55=9.1\times10^{-4}$). Although *PPARG* and *IGF2BP2* are located on the same chromosome (3p25 and 3q28, respectively), it is unlikely that loci on different arms of the same chromosome show significant linkage disequilibrium. *SLC30A8* is located on a different chromosome (8q24.11) from

PPARG. The reason why nominal *P*-values of these combinations showed less than 0.05 may be because of the low minor allele frequency of rs1801282.

Cumulative risk assessment for type 2 diabetes on the basis of susceptibility genes

As there was no evidence of gene–gene interaction between 11 SNPs of 11 genes, *SLC30A8*, *HHEX*, *CDKN2A/B*, *GCKR*, *IGF2BP2*, *CDKAL1*, *TCF7L2*, *KCNJ11*, *PPARG*, *KCNQ1* and *HNF1B*, they were included in the prediction model as independent variables with the additive effect (additive effect in the liability and multiplicative effect in the odds) without interaction terms. Effective numbers of cases and controls whose genotypes for the 11 loci were successfully obtained were 2316 and 2370, respectively. The Cochran–Armitage trend test gave a *P*-value of 4.7×10^{-56} for the trend in the increase in the odds for cases relative to controls with an increasing number of risk alleles for the 11 susceptibility loci (Supplementary Table 5). We then estimated ORs for type 2 diabetes in subjects with different numbers of risk alleles on the basis of the multiplicative model by logistic regression analysis with adjustment for age, sex and BMI. The ORs for type 2 diabetes in subjects with 7–18 risk alleles in comparison with those harboring 0–6 risk alleles are shown in Figure 1. An increase of one risk allele resulted in an average increase in the odds of 1.29 (95% CI=1.25–1.33, $P=5.4\times10^{-53}$, logistic regression analysis).

To predict disease status for type 2 diabetes in a given individual, we constructed a prediction model on the basis of the number of risk alleles or the liability value calculated from the number of risk alleles as well as age, sex and BMI. The coefficients to calculate the liability value were estimated with the logistic regression model. To estimate the predictive power of the model, we generated ROC curves as described in Materials and methods. The AUC was 0.63 when only the number of risk alleles was used for the prediction. When age, sex and BMI were also included, the AUC increased to 0.72 (Figure 2). Meanwhile, an AUC value for the ROC curve based on only age, sex and BMI was 0.68, which was better than that based on only the number of risk alleles (data now shown). The model incorporating age, sex and BMI as well as the number of risk alleles thus showed moderate power for the prediction of type 2 diabetes. The best accuracy was 0.66 at the threshold between non-diabetic and diabetic status of 0.52 (non-diabetic status=0, diabetic status=1), for which the specificity and the sensitivity were 0.71 and 0.61, respectively.

DISCUSSION

By the validation of the results from our multistage GWAS, we detected only marginal associations of *EIF2AK4*, *KRT4* and *A2BP1* with type 2 diabetes in meta-analyses with two subject panels of Japanese or Chinese individuals. Relations of *KRT4* (keratin 4 gene) and *A2BP1* (ataxin-2-binding protein 1 gene, also known as *FOX1*) to glucose or lipid metabolism are unknown. Deletion of *EIF2AK4* (eukaryotic translation initiation factor 2 alpha kinase 4 gene, also known as *GCN2*) in mice resulted in liver steatosis during leucine deprivation as a result of unrepressed expression of lipogenic genes.[30] The functionally related gene, *EIF2AK3* (also known as *PERK* or *PEK*), has been shown to cause diabetes mellitus both in humans (Wolcott–Rallison syndrome, OMIM604032) and in rodent models.[31,32] Taken together, *EIF2AK4* may be a good candidate for the diabetes susceptibility gene. The sample size required for a statistical power of 0.80 with equal numbers of cases and controls is 10 505 when the frequency of the risk allele, OR and type I error probability are assumed to be 0.20, 1.10 (the value for *EIF2AK4* in the meta-analysis in Table 1) and 0.05, respectively. Further studies of these genes in other Asian populations as well as in other ethnic groups are needed for confirmation of their association with type 2 diabetes. Given this uncertainty, we did not include these genes in the assessments of cumulative risk and gene–gene interaction.

Among tens of type 2 diabetes susceptibility genes identified by recent GWASs in Caucasians, the associations of six genes, that is, *TCF7L2*, *CDKAL1*, *CDKN2A/B*, *IGF2BP2*, *SLC30A8* and *HHEX*, have been replicated in Asian populations as well as in populations of European ancestry. A recent meta-analysis in Japanese subjects also supported the associations.[12] In this study, we performed replication study, and, on the basis of the results, we added five more genes, that is, *KCNJ11*, *PPARG*, *GCKR*, *KCNQ1* and *HNF1B*, for the cumulative risk assessment for type 2 diabetes. Thus, the SNPs of *HNF1B*, which were earlier associated with type 2 diabetes in Chinese as well as in Caucasians,[26] showed the association with the disease in the Japanese

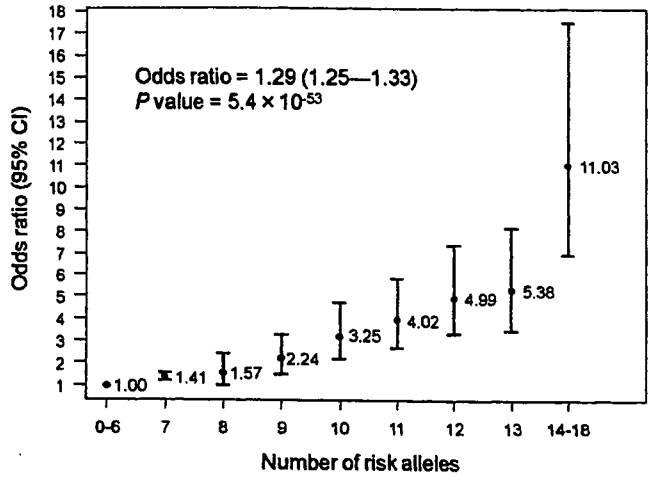

Figure 1 Odds ratios for subjects with different numbers of risk alleles for 11 susceptibility loci for type 2 diabetes. The cumulative effect of the 11 loci on type 2 diabetes was tested by counting the number of risk alleles associated with type 2 diabetes with a logistic regression model with adjustment for age, sex and BMI. The ORs for subjects with each number of risk alleles are expressed relative to individuals with 0–6 risk alleles.

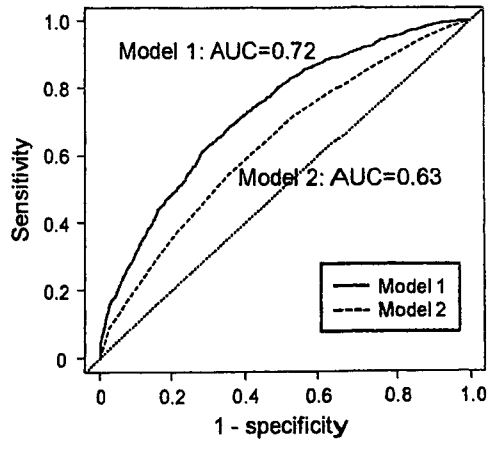

Figure 2 ROC curves for the prediction model on the basis of the number of risk alleles for 11 susceptibility loci for type 2 diabetes. The prediction model for type 2 diabetes was constructed using the logistic regression model, and ROC curves for the model were generated. In model 1, the number of risk alleles was used as an independent variable together with age, sex and BMI as covariates, whereas only the number of risk alleles was used as an independent variable in model 2.

population in this study. In addition, the *C* allele of rs780094 in *GCKR* was associated with increased risk of type 2 diabetes in this study, which is consistent with a recent study in Caucasians.[33] The associations of *KCNJ11* and *PPARG* with diabetes were marginal in this study; however, they were included for the prediction model, as the associations were replicated in some studies of Caucasians.

Our gene–gene interaction analysis showed no significant interaction for any of the 55 possible pairs of genes when corrected for multiple testing. When the significance level was set at 0.05, two pairs were judged to be significant. However, such gene–gene interactions were not supported from the functional point of view. A large-scale study may provide more convincing evidence for such interactions.

As no confirmatory evidence for gene–gene interaction was observed, we treated the 11 genes as independent variables in the prediction model. The addition of one risk allele was estimated to increase the odds by an average of 1.29 according to the multiplicative model. This value is similar to that (1.24) estimated for type 2 diabetes in Caucasians.[17] Two earlier cumulative risk assessments for type 2 diabetes in Asian populations with relatively small numbers of associated loci yielded values of 1.17 and 1.24 for the fold increase in risk for each additional risk allele.[11,34] In our prediction model for type 2 diabetes, the AUC for the ROC curve was lower than that in the earlier study[17] based on 15 loci in Caucasians (0.72 and 0.86, respectively). However, the number of loci in our study (11 loci) was lower than that in the study for Caucasians. The inclusion of additional loci in our model should improve its ability to predict type 2 diabetes in Asian populations. Several reports of the prediction of type 2 diabetes using ~18 loci were recently described for populations of European ancestry.[35–38] A prediction based on 18 loci gave an AUC value of 0.80 for the ROC curve,[35] whereas the corresponding values for a population-based prospective study were 0.68,[36] 0.615[37] and 0.75.[38] They concluded that genetic variations associated with diabetes had a small effect on the ability to predict the development of type 2 diabetes as compared with clinical characteristics alone. In fact, the AUC value (0.72) based on both the genetic variations and the clinical characteristics was slightly better than that based on only the clinical characteristics (0.68). We admit that the evidence of the association with diabetes is a little weaker for *KCNJ11* and *PPARG* in the Japanese population than for the other nine genes. If *KCNJ11* and *PPARG* were excluded from the analysis, the AUC for the ROC curve in the prediction model incorporating age, sex and BMI remained unchanged at 0.72, probably because of the relatively large effects of *KCNQ1* and *TCF7L2*.

Finally, our prediction model for type 2 diabetes achieved limited success even though it has some value. Given that GWASs for diabetes in Asians have not been as extensive as those in Caucasians, many risk loci for diabetes in Asians remain most likely to be undiscovered. Considering that the average increase in OR conferred by each additional risk allele was similar between Caucasians and Japanese, incorporation of data from additional risk loci is most likely to increase the predictive power.

ACKNOWLEDGEMENTS

We thank all the subjects who joined this project; Sumio Sugano and Shoji Tsuji for support and helpful discussion throughout the project; and Megumi Yamaoka-Sageshima for technical assistance. This work was supported by a grant from the Program for Promotion of Fundamental Studies in Health Sciences of the Pharmaceuticals and Medical Devices Agency (PMDA) of Japan; a grant from the National Institute of Biomedical Innovation (NIBIO) of Japan; grants from the Ministry of Health, Labour and Welfare of Japan; a Grant-in-Aid for Scientific Research on Priority Areas (C), 'Medical Genome Science (Millennium Genome Project)', 'Applied Genomics', and 'Comprehensive Genomics', from the Ministry of Education, Culture, Sports, Science and Technology of Japan; and a grant from the Cooperative Link of Unique Science and Technology for Economy Revitalization (CLUSTER, Tokushima, Japan). The Hong Kong diabetes case–control study was supported by the Hong Kong Research Grants Committee Central Allocation Scheme CUHK 1/04C.

1 Sladek, R., Rocheleau, G., Rung, J., Dina, C., Shen, L., Serre, D. *et al.* A genome-wide association study identifies novel risk loci for type 2 diabetes. *Nature* **445**, 881–885 (2007).
2 Saxena, R., Voight, B. F., Lyssenko, V., Burtt, N. P., de Bakker, P. I., Chen, H. *et al.* Genome-wide association analysis identifies loci for type 2 diabetes and triglyceride levels. *Science* **316**, 1331–1336 (2007).
3 Zeggini, E., Weedon, M. N., Lindgren, C. M., Frayling, T. M., Elliott, K. S., Lango, H. *et al.* Replication of genome-wide association signals in UK samples reveals risk loci for type 2 diabetes. *Science* **316**, 1336–1341 (2007).
4 Scott, L. J., Mohlke, K. L., Bonnycastle, L. L., Willer, C. J., Li, Y., Duren, W. L. *et al.* A genome-wide association study of type 2 diabetes in Finns detects multiple susceptibility variants. *Science* **316**, 1341–1345 (2007).
5 Steinthorsdottir, V., Thorleifsson, G., Reynisdottir, I., Benediktsson, R., Jonsdottir, T., Walters, G. B. *et al.* A variant in CDKAL1 influences insulin response and risk of type 2 diabetes. *Nat. Genet.* **39**, 770–775 (2007).
6 Miyake, K., Horikawa, Y., Hara, K., Yasuda, K., Osawa, H., Furuta, H. *et al.* Association of TCF7L2 polymorphisms with susceptibility to type 2 diabetes in 4087 Japanese subjects. *J. Hum. Genet.* **53**, 174–180 (2008).
7 Horikawa, Y., Miyake, K., Yasuda, K., Enya, M., Hirota, Y., Yamagata, K. *et al.* Replication of genome-wide association studies of type 2 diabetes susceptibility in Japan. *J. Clin. Endocrinol. Metab.* **93**, 3136–3141 (2008).
8 Horikoshi, M., Hara, K., Ito, C., Shojima, N., Nagai, R., Ueki, K. *et al.* Variations in the HHEX gene are associated with increased risk of type 2 diabetes in the Japanese population. *Diabe* **50**, 2461–2466 (2007).
9 Furukawa, Y., Shimada, T., Furuta, H., Matsuno, S., Kusuyama, A., Doi, A. *et al.* Polymorphisms in the IDE-KIF11-HHEX gene locus are reproducibly associated with type 2 diabetes in a Japanese population. *J. Clin. Endocrinol. Metab.* **93**, 310–314 (2008).
10 Omori, S., Tanaka, Y., Takahashi, A., Hirose, H., Kashiwagi, A., Kaku, K. *et al.* Association of CDKAL1, IGF2BP2, CDKN2A/B, HHEX, SLC30A8, and KCNJ11 with susceptibility to type 2 diabetes in a Japanese population. *Diabetes* **57**, 791–795 (2008).
11 Ng, M. C., Park, K. S., Oh, B., Tam, C. H., Cho, Y. M., Shin, H. D. *et al.* Implication of genetic variants near TCF7L2, SLC30A8, HHEX, CDKAL1, CDKN2A/B, IGF2BP2 and FTO in type 2 diabetes and obesity in 6719 Asians. *Diabetes* **57**, 2226–2233 (2008).
12 Tabara, Y., Osawa, H., Kawamoto, R., Onuma, H., Shimizu, I., Miki, T. *et al.* Replication study of candidate genes associated with type 2 diabetes based on genome-wide screening. *Diabetes* **58**, 493–498 (2009)10.2337/db07-1785..
13 Grarup, N., Rose, C. S., Andersson, E. A., Andersen, G., Nielsen, A. L., Albrechtsen, A. *et al.* Studies of association of variants near the HHEX, CDKN2A/B, and IGF2BP2 genes with type 2 diabetes and impaired insulin release in 10705 Danish subjects: validation and extension of genome-wide association studies. *Diabetes* **56**, 3105–3111 (2007).
14 Cauchi, S., Proença, C., Choquet, H., Gaget, S., De Graeve, F., Marre, M. *et al.* 2008 Analysis of novel risk loci for type 2 diabetes in a general French population: the D.E.S.I.R. study. *J. Mol. Med.* **86**, 341–348 (2008).
15 Yasuda, K., Miyake, K., Horikawa, Y., Hara, K., Osawa, H., Furuta, H. *et al.* Variants in KCNQ1 are associated with susceptibility to type 2 diabetes mellitus. *Nat. Genet.* **40**, 1092–1097 (2008).
16 Zeggini, E., Scott, L. J., Saxena, R., Voight, B. F., Marchini, J. L., Hu, T. *et al.* Meta-analysis of genome-wide association data and large-scale replication identifies additional susceptibility loci for type 2 diabetes. *Nat. Genet.* **40**, 638–645 (2008).
17 Cauchi, S., Meyre, D., Durand, E., Proença, C., Marre, M., Hadjadj, S. *et al.* Post genome-wide association studies of novel genes associated with type 2 diabetes show gene-gene interaction and high predictive value. *PLoS ONE* **3**, e2031 (2008).
18 Yang, X., So, W. Y., Kong, A. P., Ho, C. S., Lam, C. W., Stevens, R. J. *et al.* Development and validation of stroke risk equation for Hong Kong Chinese patients with type 2 diabetes: the Hong Kong Diabetes Registry. *Diabetes Care* **30**, 65–70 (2007).
19 Ozaki, R., Qiao, Q., Wong, G. W., Chan, M. H., So, W. Y., Tong, P. C. *et al.* Overweight, family history of diabetes and attending schools of lower academic grading are independent predictors for metabolic syndrome in Hong Kong Chinese adolescents. *Arch. Dis. Child.* **92**, 224–228 (2007).
20 Bannai, M., Higuchi, K., Akesaka, T., Furukawa, M., Yamaoka, M., Sato, K. *et al.* Single-nucleotide-polymorphism genotyping for whole-genome-amplified samples using automated fluorescence correlation spectroscopy. *Anal. Biochem.* **327**, 215–221 (2004).
21 Sing, T., Sander, O., Beerenwinkel, N. & Lengauer, T. ROCR: visualizing classifier performance in R. *Bioinformatics* **21**, 3940–3941 (2005).
22 Grant, S. F., Thorleifsson, G., Reynisdottir, I., Benediktsson, R., Manolescu, A., Sainz, J. *et al.* Variant of transcription factor 7-like 2 (TCF7L2) gene confers risk of type 2 diabetes. *Nat. Genet.* **38**, 320–323 (2006).

23 Gloyn, A. L., Weedon, M. N., Owen, K. R., Turner, M. J., Knight, B. A., Hitman, G. *et al.* Large-scale association studies of variants in genes encoding the pancreatic beta-cell KATP channel subunits Kir6.2 (KCNJ11) and SUR1 (ABCC8) confirm that the KCNJ11 E23K variant is associated with type 2 diabetes. *Diabetes* **52**, 568–572 (2003).
24 Altshuler, D., Hirschhorn, J. N., Klannemark, M., Lindgren, C. M., Vohl, M. C., Nemesh, J. *et al.* The common PPARgamma Pro12Ala polymorphism is associated with decreased risk of type 2 diabetes. *Nat. Genet.* **26**, 76–80 (2000).
25 Sandhu, M. S., Weedon, M. N., Fawcett, K. A., Wasson, J., Debenham, S. L., Daly, A. *et al.* Common variants in WFS1 confer risk of type 2 diabetes. *Nat. Genet.* **39**, 951–953 (2007).
26 Gudmundsson, J., Sulem, P., Steinthorsdottir, V., Bergthorsson, J. T., Thorleifsson, G., Manolescu, A. *et al.* Two variants on chromosome 17 confer prostate cancer risk, and the one in TCF2 protects against type 2 diabetes. *Nat. Genet.* **39**, 977–983 (2007).
27 Horikoshi, M., Hara, K., Ito, C., Nagai, R., Froguel, P. & Kadowaki, T. A genetic variation of the transcription factor 7-like 2 gene is associated with risk of type 2 diabetes in the Japanese population. *Diabetologia* **50**, 747–751 (2007).
28 Yokoi, N., Kanamori, M., Horikawa, Y., Takeda, J., Sanke, T., Furuta, H. *et al.* Association studies of variants in the genes involved in pancreatic beta-cell function in type 2 diabetes in Japanese subjects. *Diabetes* **55**, 2379–2386 (2006).
29 Mori, H., Ikegami, H., Kawaguchi, Y., Seino, S., Yokoi, N., Takeda, J. *et al.* The Pro12→Ala substitution in PPAR-gamma is associated with resistance to development of diabetes in the general population: possible involvement in impairment of insulin secretion in individuals with type 2 diabetes. *Diabetes* **50**, 891–894 (2001).
30 Guo, F. & Cavener, D. R. The GCN2 eIF2alpha kinase regulates fatty-acid homeostasis in the liver during deprivation of an essential amino acid. *Cell Metab.* **5**, 103–114 (2007).
31 Harding, H. P., Zeng, H., Zhang, Y., Jungries, R., Chung, P., Plesken, H. *et al.* Diabetes mellitus and exocrine pancreatic dysfunction in Perk$^{-/-}$ mice reveals a role for translational control in secretory cell survival. *Mol. Cell.* **7**, 1153–1163 (2001).
32 Delépine, M., Nicolino, M., Barrett, T., Golamaully, M., Lathrop, G. M. & Julier, C. EIF2AK3, encoding translation initiation factor 2-alpha kinase 3, is mutated in patients with Wolcott–Rallison syndrome. *Nat. Genet.* **25**, 406–409 (2000).
33 Sparsø, T., Andersen, G., Nielsen, T., Burgdorf, K. S., Gjesing, A. P., Nielsen, A. L. *et al.* The GCKR rs780094 polymorphism is associated with elevated fasting serum triacylglycerol, reduced fasting and OGTT-related insulinaemia, and reduced risk of type 2 diabetes. *Diabetologia* **51**, 70–75 (2008).
34 Wu, Y., Li, H., Loos, R. J., Yu, Z., Ye, X., Chen, L. *et al.* Common variants in CDKAL1, CDKN2A/B, IGF2BP2, SLC30A8 and HHEX/IDE genes are associated with type 2 diabetes and impaired fasting glucose in a Chinese Han population. *Diabetes* **57**, 2834–2842 (2008).
35 Lango, H., Palmer, C. N., Morris, A. D., Zeggini, E., Hattersley, A. T., McCarthy, M. I., *et al.* The UK Type 2 Diabetes Genetics Consortium Assessing the combined impact of 18 common genetic variants of modest effect sizes on type 2 diabetes risk. *Diabetes* **57**, 3129–3135 (2008).
36 van Hoek, M., Dehgan, A., Witteman, J. C., van Duijn, C. M., Uitterlinden, A. G., Oostra, B. A. *et al.* Predicting type 2 diabetes based on polymorphisms from genome wide association studies: a population-based study. *Diabetes* **57**, 3122–3128 (2008).
37 Meigs, J. B., Shrader, P., Sullivan, L. M., McAteer, J. B., Fox, C. S., Dupuis, J. *et al.* Genotype score in addition to common risk factors for prediction of type 2 diabetes. *N Engl J Med.* **359**, 2208–2219 (2008).
38 Lyssenko, V., Jonsson, A., Almgren, P., Pulizzi, N., Isomaa, B., Tuomi, T. *et al.* Clinical risk factors, DNA variants, and the development of type 2 diabetes. *N. Engl. J. Med.* **359**, 2220–2232 (2008).

Supplementary Information accompanies the paper on Journal of Human Genetics website (http://www.nature.com/jhg)

INTERNAL MEDICINE

□ CASE REPORT □

Peginterferon (PEG-IFN) Plus Ribavirin Combination Therapy, but neither Interferon nor PGE-IFN Alone, Induced Type 1 Diabetes in a Patient with Chronic Hepatitis C

Takehide Ogihara[1], Hideki Katagiri[1], Tetsuya Yamada[1], Hirohito Kudo[1], Junta Imai[1], Yasushi Ishigaki[1], Yoshinori Hinokio[1], Yoko Yamagiwa[2], Yoshiyuki Ueno[2], Tooru Shimosegawa[2] and Yoshitomo Oka[1]

Abstract

Interferon (IFN) therapies, including IFN, peginterferon (PEG-IFN) and ribavirin (RBV) plus PEG-IFN combination, are widely used for patients with chronic hepatitis C. We encountered a patient with chronic hepatitis C in whom previous IFN or PEG-IFN alone had not induced type 1 diabetes (T1D), while the addition of RBV to PEG-IFN did induce T1D. The patient had HLA types conferring highly susceptibility to T1D. Thus, adding RBV to PEG-IFN may render chronic hepatitis C patients, with T1D-susceptible HLA types, more prone to developing T1D than IFN or PEG-IFN alone. To prevent T1D development, we recommend HLA typing prior to initiating RBV plus PEG-IFN administration.

Key words: human leukocyte antigen, anti-glutamate acid decarboxylase (GAD) antibody, anti-insulinoma-associated antigen (IA)-2 antibody, autoimmune disease

(Inter Med 48: 1387-1390, 2009)
(DOI: 10.2169/internalmedicine.48.2220)

Introduction

Interferon (IFN) is used for chronic hepatitis C and B. Until recently, IFNα was the main option for treating chronic hepatitis C (1). Now, peginterferon (PEG-IFN, polyethylene glycol-binding IFN) combined with ribavirin (RBV), which augments IFN action, is a standard anti-viral therapy for chronic hepatitis C (2). However, IFN therapy can adversely impact the immune system and induce autoimmune diseases including type 1 diabetes (T1D) (3, 4). Not only IFN, but also PEG-IFN (5) and PEG-IFN plus RBV therapy (6, 7), can reportedly induce T1D. We encountered a patient with chronic hepatitis C in whom neither IFN nor PEG-IFN alone induced T1D, while RBV plus PEG-IFN did induce T1D with elevated anti-glutamate acid decarboxylase (GAD) and anti-insulinoma-associated antigen (IA)-2 antibodies. Herein, we emphasize the risk of T1D development with PEG-IFN plus RBV therapy.

Case Report

A woman was diagnosed as having chronic hepatitis C at the age of 53 and received IFNα 1 million IU/week for 6 months, and subsequently became negative for viral marker (HCV-RNA). At age 60, she was diagnosed as having type 2 diabetes; fasting plasma glucose (FPG) was 199 mg/dL and HbA1c 6.9%. Her HbA1c improved with glimepiride 1 mg/day. Because HCV-RNA was again increased, PEG-IFNα 180 μg/week was started at age 61. Due to a taste disorder, the dose was decreased to 90 μg/week two months later and continued for 9 months. During PEG-IFN administration, blood glucose control worsened, but adding buformin (150 mg/day) to her treatment regimen decreased HbA1c from

[1]Department of Diabetes and Metabolism, Tohoku University Hospital, Sendai and [2]Department of Gastroenterology, Tohoku University Hospital, Sendai

Received for publication February 27, 2009; Accepted for publication April 6, 2009

Correspondence to Dr. Yoshitomo Oka, oka-y@mail.tains.tohoku.ac.jp

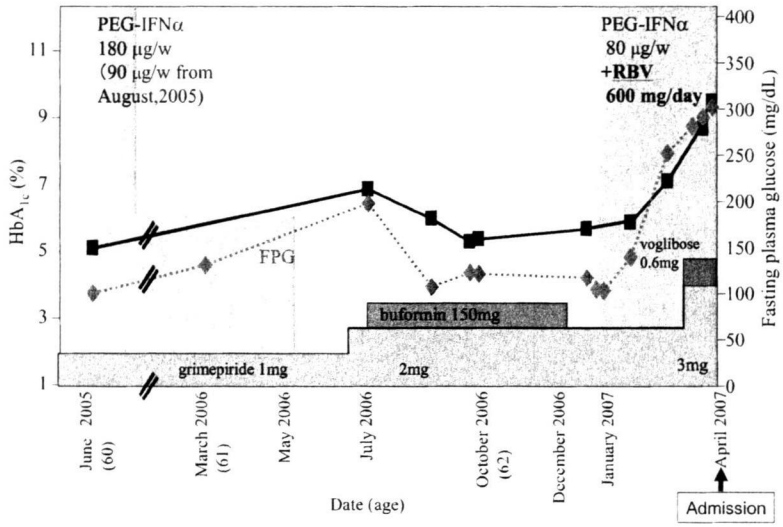

Figure 1. Clinical course: HbA_{1c} and fasting plasma glucose.

Table 1. Data on Admission

WBC	1600 /μL	T-Bil	0.9 mg/dL	BUN	11 mg/dL	Glu	303 mg/dL
Seg	53 %	AST	53 IU/L	Cr	0.4 mg/dL	HbA1c	9.5 %
Eos	2 %	ALT	60 IU/L	UA	2.3 mg/dL	Anti-GAD antibody	27.0 U/mL (0-1.4)
Baso	0 %	ALP	213 IU/L	Na	135 mEq/L	Anti-IA-2 antibody	3.0 U/mL (0-0.3)
Lym	34 %	γ-GTP	40 IU/L	K	4.1 mEq/L	Anti-insulin antibody	6.5 % (0-10)
Mon	11 %	LDH	195 IU/L	Cl	102 mEq/L	Fasting IRI	4.3 μU/mL(1.84-12.2)
RBC	326×10^4 /μL	ZTT	10.2 U	Ca	8.7 mg/dL	Blood C-peptide	0.6 ng/mL (1.5-3.5)
Hb	10.7 g/dL	TTT	6.1 U	TG	54 mg/dL	Urinary C-peptide	25.0 μg/day (41-145)
Ht	31.3 %	CHE	304 IU/L	T-Cho	78 mg/dL	Free T3	2.6 pg/mL (2.5-4.3)
Plt	78×10^4 /μL	CPK	25 IU/L	HDL-C	27 mg/dL	Free T4	0.91 ng/mL (1.76-1.65)
TP	6.7 g/dL			LDL-C	39 mg/dL	TSH	6.72 μIU/mL (0.31-4.69)
A/G	1.48					TRAb	2.1 % (<15%)
						TgAb	138.2 IU/mL (0-44)
						TPOAb	149.9 IU/mL (<0.72)

Normal ranges are in parenthesis

7.0% to 5.0%. At age 62, because HCV-RNA levels had not decreased, PEG-IFN (80 μg/week) plus RBV (600 mg/day) combination therapy was started. Glycemic control rapidly deteriorated; FPG and HbA1c were increased to 280 mg/dL and 8.8%, respectively, two months after the initiation of RBV therapy (Fig. 1). One month later, the patient was admitted to our hospital for blood glucose control. On admission, her body mass index was 20.8 kg/m^2, with no remarkable physical findings. Laboratory data included high blood glucose (FPG 303 mg/dL, HbA1c 9.5%) with slightly elevated hepatic transaminases (AST/ALT 53/60 IU/L). It was noteworthy that she was positive for both anti-GAD and anti-IA2 antibodies. Thyroid hormone levels were normal with slightly elevated TSH. Anti-thyroglobulin antibody (TbAb) and anti-thyroid peroxidase antibody (TPOAb) were positive (Table 1), suggesting autoimmune thyroiditis with subclinical hypothyroidism. Her HLA types included A24, DRB1*0405/0901, DQA1*0302 and DQB1*0401/0303, which confer high susceptibility to T1D. Based on positive autoantibodies against pancreatic islets, T1D was diagnosed. The PEG-IFN and RBV combination therapy was stopped and intensive insulin therapy was started, resulting in gradual improvement of blood glucose control with 35 units/day of insulin. Five months later, anti-GAD antibody remained positive (31.7 U/mL) with fair blood glucose control (HbA1c 5.5%) using 27 units/day of insulin.

Discussion

Since IFN was first reported to be effective for HCV infection in 1986 (8), IFN has been widely used for patients with chronic hepatitis C. However, autoimmune diseases, such as autoimmune thyroiditis (9), rheumatoid arthritis (10), autoimmune hepatitis (11), systemic lupus erythematosus (12) and T1D (13), reportedly develop with IFN therapy. In particular, several reports have documented the development of thyroid autoimmune disorders in cases receiving IFN plus RBV combination therapy (14, 15) and the present patient is likely such a case.

T1D is at least in part an autoimmune disease character-

ized by loss of pancreatic β cells with T lymphocyte infiltration of islets (16). IFNα activates T-helper (Th)1 lymphocytes which are $CD4^+$ and secrete interleukin-2, IFNγ and tumor necrosis factor β. These cytokines facilitate the generation of $CD8^+$ cytotoxic T cells which injure pancreatic β cells (17). In fact, IFNα is significantly up-regulated in patients with T1D (18). These findings suggest that IFNα is involved in β cell destruction and thereby in T1D development.

In 1992, it was documented for the first time that IFN therapy for chronic hepatitis C can induce T1D (13), and this was followed by similar case reports (reviewed in (19)). Subsequently, PEG-IFN therapy was also reported to induce T1D (5). Therefore, IFN administration is likely to affect Th1 immune reactions, leading to the development of T1D, as discussed above.

The present case was first diagnosed as having type 2 diabetes 7 years after IFN therapy. IFN therapy reportedly worsens insulin resistance, resulting in deterioration of glucose tolerance (20). In our case as well, blood glucose control deteriorated slightly during PEG-IFN therapy, though fair control of blood glucose was achieved with biguanide treatment but no insulin, indicating that the diabetes in this case was not clinically insulin-dependent T1D during this period. In contrast, after RBV was added to PEG-IFN, glucose control rapidly worsened with positive autoantibodies, i.e. anti-GAD and anti-IA2 antibodies, suggesting T1D onset. Although the possibility that IFN or PEG-IFN alone had induced T1D several years or months earlier can not be completely excluded in this patient, her clinical course (see Fig. 1) strongly suggests that the RBV addition was a trigger for T1D development.

It is likely that previous administrations of IFN and PEG-IFN alone had not induced T1D, while adding RBV to PEG-IFN had induced T1D in the same patient. These three anti-viral strategies for chronic hepatitis C can all reportedly induce T1D (3-7). To our knowledge, however, no studies have compared these three therapies in terms of the likelihood of T1D induction. The clinical course of our case strongly suggests that adding RBV renders patients, who have T1D-susceptible HLA, more prone to T1D development than either IFN or PEG-IFN alone. RBV is a guanosine analog which exerts immunological effects on Th1-like activation (21). Therefore, adding RBV to IFN therapy might augment the autoimmune response to IFN. We emphasize the importance of HLA typing, particularly prior to RBV addition, since the combination of PEG-IFN with RBV is now established as the first line therapy for chronic hepatitis C (22, 23). RBV administration should be avoided in patients with T1D-susceptible HLA.

References

1. Hoofnagle JH, di Bisceglie AM. The treatment of chronic viral hepatitis. N Engl J Med **336**: 347-356, 1997.
2. Mangia A, Santoro R, Minerva N, et al. Peginterferon alfa-2b and ribavirin for 12 vs. 24 weeks in HCV genotype 2 or 3. N Engl J Med **352**: 2609-2617, 2005.
3. Shiba T, Morino Y, Tagawa K, Fujino H, Unuma T. Onset of diabetes with high titer anti-GAD antibody after IFN therapy for chronic hepatitis. Diabetes Res Clin Pract **30**: 237-241, 1995.
4. Uto H, Matsuoka H, Murata M, et al. A case of chronic hepatitis C developing insulin-dependent diabetes mellitus associated with various autoantibodies during interferon therapy. Diabetes Res Clin Pract **49**: 101-106, 2000.
5. Schreuder TC, Gelderblom HC, Weegink CJ, et al. High incidence of type 1 diabetes mellitus during or shortly after treatment with pegylated interferon alpha for chronic hepatitis C virus infection. Liver Int **28**: 39-46, 2008.
6. Cozzolongo R, Betterle C, Fabris P, Paola Albergoni M, Lanzilotta E, Manghisi OG. Onset of type 1 diabetes mellitus during peginterferon alpha-2b plus ribavirin treatment for chronic hepatitis C. Eur J Gastroenterol Hepatol **18**: 689-692, 2006.
7. Tanaka J SK, Shiraki K, Beppu T, et al. Type 1 diabetes mellitus proveked by peginterferon alpha-2b plus ribavirin treatment for chronic hepatitis C. Inter Med **47**: 747-749, 2008.
8. Hoofnagle JH, Mullen KD, Jones DB, et al. Treatment of chronic non-A, non-B hepatitis with recombinant human alpha interferon. A preliminary report. N Engl J Med **315**: 1575-1578, 1986.
9. Gisslinger H, Gilly B, Woloszczuk W, et al. Thyroid autoimmunity and hypothyroidism during long-term treatment with recombinant interferon-alpha. Clin Exp Immunol **90**: 363-367, 1992.
10. Nadir F, Faqiuoli S, Wright HI, et al. Rheumatoid arthritis: a complication of interferon therapy. J Okla State Med Assoc **87**: 228-230, 1994.
11. Papo T, Marcellin P, Bernuau J, Durand F, Poynard T, Benhamou JP. Autoimmune chronic hepatitis exacerbated by alpha-interferon. Ann Intern Med **116**: 51-53, 1992.
12. Schilling PJ, Kurzrock R, Kantarjian H, Gutterman JU, Talpaz M. Development of systemic lupus erythematosus after interferon therapy for chronic myelogenous leukemia. Cancer **68**: 1536-1537, 1991.
13. Fabris P, Betterle C, Floreani A, et al. Development of type 1 diabetes mellitus during interferon alfa therapy for chronic HCV hepatitis. Lancet **340**: 548, 1992.
14. Parana R, Cruz M, Lyra L, Cruz T. Subacute thyroiditis during treatment with combination therapy (interferon plus ribavirin) for hepatitis C virus. J Viral Hepat **7**: 393-395, 2000.
15. Harris DM, Hespenheide EE, Dalkin AC, Kirk SE, Ellis DS, Caldwell SH. Hyperthyroidism with interferon-ribavirin therapy for hepatitis C: a case report and proposed treatment algorithm. Am J Gastroenterol **95**: 2995-2996, 2000.
16. Bottazzo GF, Dean BM, McNally JM, MacKay EH, Swift PG, Gamble DR. In situ characterization of autoimmune phenomena and expression of HLA molecules in the pancreas in diabetic insulitis. N Engl J Med 353-360, 1985.
17. Chakrabarti D, Hultgren B, Stewart TA. IFN-alpha induces autoimmune T cells through the induction of intracellular adhesion molecule-1 and B7.2. J Immunol **157**: 522-528, 1996.
18. Huang X, Yuang J, Goddard A, et al. Interferon expression in the pancreases of patients with type I diabetes. Diabetes **44**: 658-664, 1995.
19. Fabris P, Floreani A, Tositti G, Vergani D, De Lalla F, Betterle C. Type 1 diabetes mellitus in patients with chronic hepatitis C before and after interferon therapy. Aliment Pharmacol Ther **18**: 549-558, 2003.
20. Koivisto VA, Pelkonen R, Cantell K. Effect of interferon on glucose tolerance and insulin sensitivity. Diabetes **38**: 641-647, 1989.
21. McHutchison JG, Gordon SC, Schiff ER, et al. Interferon alfa-2b

alone or in combination with ribavirin as initial treatment for chronic hepatitis C. Hepatitis Interventional Therapy Group. N Engl J Med **339**: 1485-1492, 1998.

22. Davis GL, Esteban-Mur R, Rustgi V, et al. Interferon alfa-2b alone or in combination with ribavirin for the treatment of relapse of chronic hepatitis C. International Hepatitis Interventional Therapy Group. N Engl J Med **339**: 1493-1499, 1998.

23. Tam RC, Pai B, Bard J, et al. Ribavirin polarizes human T cell responses towards a Type 1 cytokine profile. J Hepatol **30**: 376-382, 1999.

Islets 1:1, 73-75; July/August 2009; © 2009 Landes Bioscience

Identification of a novel mechanism regulating β-cell mass

Neuronal relay from the liver to pancreatic β-cells

Junta Imai,[1] Yoshitomo Oka[1] and Hideki Katagiri[2,*]

Divisions of [1]Molecular Metabolism and Diabetes; and [2]Advanced Therapeutics for Metabolic Diseases; Center for Translational and Advanced Animal Research; Tohoku University Graduate School of Medicine; Sendai, Japan

Key words: compensatory β-cell response, β-cell proliferation, regenerative medicine, diabetes, insulin, inter-organ metabolic communication, neuronal relay, insulin resistance

Submitted: 03/31/09
Accepted: 04/01/09

Previously published online:
www.landesbioscience.com/journals/islets/article/8615

Correspondence to:
Hideki Katagiri; Email: katagiri@mail.tains.tohoku.ac.jp

Addendum to: Imai J, Katagiri H, Yamada T, Ishigaki Y, Suzuki T, Kudo H, et al. Regulation of pancreatic β-cell mass by neuronal signals from the liver. Science 2008; 322:1250-4; PMID: 19023081; DOI: 10.1126/science.1163971.

Recent studies have demonstrated that β-cell replication plays a central role in maintaining adult β-cell mass. β-cell proliferative activity changes dynamically to meet systemic needs throughout life. One condition in which β-cell proliferation is enhanced is obesity-related insulin resistance. However, the mechanism underlying this compensatory β-cell response is not well understood. We have identified a neuronal relay, originating in the liver, which enhances both insulin secretion and pancreatic β-cell proliferation. Blockade of this neural relay in murine obesity models inhibited pancreatic islet expansion during obesity development, showing this inter-organ communication system to be physiologically involved in compensatory β-cell proliferation. While there is controversy about which mechanism, proliferation of pre-existing β-cells or production of new β-cells from progenitor cells, plays the dominant role in maintaining or regulating β-cell mass, we herein provide an example that proliferation of pre-existing β-cells contributes to a β-cell increment in obesity-related insulin resistance. Furthermore, we have shown the potential for clinical application of this inter-organ system as a therapeutic target for insulin-deficient diabetes.

Although pancreatic β-cells were once thought to be incapable of significant proliferation due to being in a terminal differentiation state, recently derived evidence has revealed that β-cell replication plays a central role in maintaining adult β-cell mass.[1] In addition, rates of β-cell proliferation change dynamically according to metabolic demand throughout life.[2] Proliferation of β-cells occurs at a high rate during the late embryonic stage, but begins to decline postnatally. During adulthood, though β-cells continue proliferating, the rate of proliferation gradually declines with age.[3] However, even during adulthood, proliferation rates of β-cells can increase considerably under specific conditions such as pregnancy or obesity. Enhancement of β-cell proliferation under such conditions is regarded as a compensatory mechanism in response to increasing systemic insulin demand. Although important roles of insulin[4] and glucose[5] in this β-cell compensation have been suggested, the mechanism underlying this process is not well understood. In fact, insulin-resistant animals[6,7] and human subjects[8] reportedly exhibit islet hyperplasia and/or hyperinsulinemia prior to the onset of detectable hyperglycemia, suggesting the existence of as yet unknown mechanisms enhancing compensatory β-cell proliferation in response to obesity-related insulin resistance.

Metabolism does not occur independently in multiple organs, but rather in a coordinated and regulated manner. This coordinated metabolic regulation requires inter-organ metabolic communication. During this decade, growing evidence has suggested an essential role of this inter-organ communication system in maintaining systemic metabolism, and that impairment of this system apparently contributes to the pathogenesis of metabolic disorders.[9] While humoral factors such as cytokines or nutrients are known to be important mediators of inter-organ

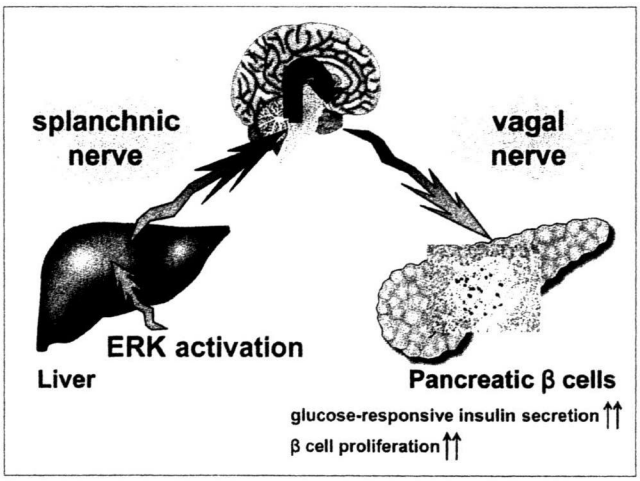

Figure 1. Schematic model of the neuronal relay originating in the liver.

communication, recent reports, including ours, have identified that neuronal signaling, consisting of both afferent and efferent autonomic nerves, also plays important roles in this system.[10] For instance, neuronal afferent signals from visceral adipose tissue modulate food intake,[11] those from the liver regulate systemic energy expenditure,[12] and sympathetic nerves regulate adiponectin synthesis in white adipose tissues.[13] In addition to these mechanisms, we have further unraveled that pancreatic β-cells are also regulated by in the nerve-mediated inter-organ communication system.[14]

To elucidate the mechanisms underlying these compensatory responses of β-cells, we expressed several genes, known to be upregulated or activated in the livers of obesity models, in the livers of lean mice. Among them, we found that hepatic extracellular signal-regulated kinase (ERK), phosphorylation of which is reportedly enhanced in the liver of a murine obesity model,[15,16] plays an important role in compensatory β-cell responses. To elucidate the metabolic roles of hepatic ERK activation, we expressed the constitutively active mutant of mitogen-activated protein kinase/ERK kinase (MEK-1) in the liver using an adenoviral gene transduction system.[17] Intriguingly, liver-selective ERK activation induced insulin hypersecretion and β-cell proliferation. These pancreatic effects of hepatic ERK activation were inhibited by splanchnic afferent blockade, pancreatic vagus dissection or midbrain transection. These results indicate that a neuronal relay system, consisting of the afferent splanchnic nerve, the central nervous system and the efferent vagus, mediates inter-organ (liver-to-pancreas) communication (**Fig. 1**). In addition, blockade of this neuronal relay at each of several steps in murine obesity models inhibited pancreatic islet expansion during obesity development, showing that this novel inter-organ communication system is physiologically involved in compensatory β-cell proliferation. Furthermore, it is noteworthy that, when applied to murine models of insulin-deficient diabetes, hepatic activation of ERK signaling induced β-cell regeneration and thereby improved diabetes.

This inter-organ machinery has been shown to physiologically elicit compensatory β-cell responses to obesity-related insulin resistance, and may thus function as a diabetes prevention system during obesity development. When systemic insulin demand is increased, it may be reasonable for animals to enhance glucose-responsive insulin secretion from preexisting β-cells in the early period and, subsequently to augment β-cell mass to later sustain insulin secretion. It is noteworthy that these sequential responses of β-cells are very similar to responses observed after activation of the hepatic ERK pathway, enhancing insulin secretion and augmenting β-cell mass during the early and late periods after hepatic ERK activation, respectively. Thus, activation of this inter-organ machinery is a possible candidate for the currently unknown trigger initiating compensatory β-cell responses.

We do not deny the possibility that progenitor cells contribute to the β-cell increment under certain conditions. In fact, we reported that bone marrow transplantation following pharmacological β-cell injury increased pancreatic islets in the vicinity of pancreatic ducts with a substantial increment in proliferating ductal cells,[18] suggesting generation of new islets from ductal progenitor cells. However, after activation of the hepatic ERK pathway, β-cell proliferation was tremendously increased within islets, suggesting that self-duplication of pre-existing β-cells is the main source of β-cell increments in this system. We performed further experiments to explore whether new β-cells were derived from progenitor cells or pre-existing β-cells proliferating in the context of inter-organ communication. We activated the hepatic ERK pathways of mice in which β-cells had been more thoroughly obliterated than in the experiments described in our original article, by administering a higher dose of streptozotocin. In these mice, pancreatic insulin contents were only slightly increased (from 6 to 9 ng/mg pancreas), indicating that the therapeutic effect of hepatic ERK activation depends on the remaining β-cell mass. Thus, increments in pancreatic insulin contents appear to be attributable to self-duplication of pre-existing β-cells. There is controversy about which mechanism, proliferation of pre-existing β-cells[1,19] or the production of new β-cells from progenitor cells,[20] plays the major role in regulating β-cell mass under both physiological and pathological conditions. We have provided an example, supporting the notion that proliferation of pre-existing β-cells contributes to β-cell increments, at least under one major pathological condition, obesity-related insulin resistance.

We would like to emphasize the potential therapeutic application of this inter-organ communication to insulin-deficient diabetes. Type 1 diabetes mellitus is characterized by progressive loss of β-cells, leading to a life-long dependence on insulin treatments. Recently, β-cells were also reported to be decreased in type 2 diabetes.[21] In such patients, one potential underlying mechanism is β-cell apoptosis induced by endoplasmic reticulum (ER) stress.[22-24] In this study, we succeeded in improving both types of insulin-deficient